Available online at www.sciencedirect.com
SCIENCE DIRECT
Cement and Concrete Research 35 (2005) 2116 – 2136
Cement and Concrete Research

# Self-Compacting Concrete: Theoretical and experimental study

H.J.H. Brouwers *, H.J. Radix

*Department of Civil Engineering, Faculty of Engineering Technology, University of Twente, P.O. Box 217, 7500 AE Enschede, The Netherlands*

Received 11 August 2004; accepted 9 June 2005

**Abstract**

This paper addresses experiments and theories on Self-Compacting Concrete. First, the features of "Japanese and Chinese Methods" are discussed, in which the packing of sand and gravel plays a major role. Here, the grading and packing of all solids in the concrete mix serves as a basis for the development of new concrete mixes. Mixes, consisting of slag blended cement, gravel (4–16 mm), three types of sand (0–1, 0–2 and 0–4 mm) and a polycarboxylic ether type superplasticizer, were developed. These mixes are extensively tested, both in fresh and hardened states, and meet all practical and technical requirements such as medium strength and low cost. It follows that the particle size distribution of all solids in the mix should follow the grading line as presented by Andreasen and Andersen. Furthermore, the packing behaviour of the powders (cement, fly ash, stone powder) and aggregates (three sands and gravel) used are analysed in detail. It follows that their loosely piled void fraction are reduced to the same extent (23%) upon vibration (aggregates) or mixing with water (powders). Finally, the paste lines of the powders are used to derive a linear relation between the deformation coefficient and the product of Blaine value and particle density.


*Keywords:* High-Performance Concrete; Particle size distribution; Mixture proportioning; Workability; Mechanical properties

## 1. Introduction

The development of Self-Compacting Concrete (SCC), also referred to as "Self-Consolidating Concrete" and "High-Performance Concrete", has recently been one of the most important developments in the building industry. It is a kind of concrete that can flow through and fill gaps of reinforcement and corners of moulds without any need for vibration and compaction during the pouring process. It can be used in pre-cast applications or for concrete placed on site. SCC results in durable concrete structures, and saves labour and consolidation noise. Pioneering work in the development of SCC was carried out by Okamura [1] and Okamura and Ouchi [2], which will henceforth be referred to as Japanese Method. The method suggests that the gravel content in the concrete mix corresponds to 50% of its packed density, and that in the mortar the sand content corresponds to about 50% of its packed density (Fig. 1). This independent consideration of gravel and sand, results in SCC that has a relatively high content of paste. Many SCC mixes therefore attain a higher strength than actually required [3,4]. In the Netherlands, and many other European countries, the Japanese Method has been adopted and used as a starting point for the development of SCC [5].

More recently, Su et al. [6] and Su and Miao [7] developed an alternative method for composing SCC, henceforth referred to as Chinese Method. The Chinese Method starts with the packing of all aggregates (sand and gravel together), and later with the filling of the aggregate voids with paste. The method is easier to carry out, and results in less paste. This saves the most expensive constituents, namely cement and filler, and concrete of "normal" strength is obtained. This will also favour the technical performance of the concrete, as the largest possible volume of aggregate is advantageous in regard to strength, stiffness, permeability, creep and drying shrinkage.

First, this Chinese Method is discussed in detail and applied to the Dutch (or European) situation such as available constituents, prevailing standards, etc. As aggre-

* Corresponding author.
*E-mail address:* h.j.h.brouwers@utwente.nl (H.J.H. Brouwers).

0008-8846/$ - see front matter © 2005 Elsevier Ltd. All rights reserved.
doi:10.1016/j.cemconres.2005.06.002

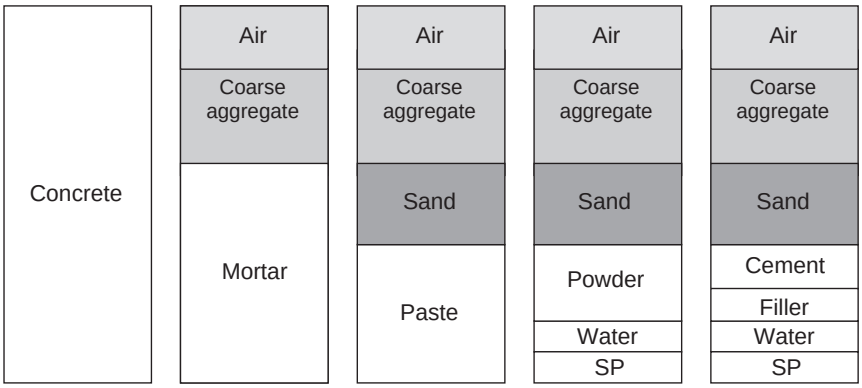


Fig. 1. Schematic composition of SCC (Ernst [5]).

gate is the cheapest component, attention will first be paid to the optimum packing of this component in the mix. Using mix of gravel and three types of sand (all quartz), optimum packing in loose and compacted states is investigated. The three sands comprise coarse sand (0–4 mm, "concrete sand"), medium sand (0–2 mm, "masonry sand") and fine sand (0–1 mm). At present, the fine sand is hardly used in concrete products and considered as "waste", its price is about 3/4 the price of masonry sand and only half the price of concrete sand in The Netherlands. Next, the filler and the cement are considered. Following the Japanese and Chinese Methods, paste lines are measured for relevant water–powders (cement, fly ash, stone powder). A general relation is derived between the packing and specific surface area of each powder on the one hand, and the water required for flowing and slumps on the other hand.

Though, with both Japanese and Chinese methods, SCC can be composed, a thorough theoretical background is still lacking, which is also addressed in this paper. Starting point of this analysis is the packing theory. SCC is treated as a mix of water and solids, whereby the solids consist (from coarse to fine) of gravel, sand, filler (stone powder, fly ash) and cement. The relation between packing and concrete properties is generally known, and usually a grading curve is selected for the aggregate [8]. This grading comprises the fine aggregate and goes down to a particle size of typically 150 μm. In order to model the concrete mix, all solids should be considered, so also the cement and the filler.

Regard the packing of granular materials, Andreasen and Andersen [9] presented a semi-empirical study of the packing of continuous particle size distributions (PSD), and determined the PSD with the densest packing. Funk and Dinger [10] modified this PSD to account for the smallest particle size (modified A&A model). Using this PSD, they were able to make coal–water slurries with a solid content as high as 80% and with viscosities of about 300 mPas. This confirms the positive relationship between rheological properties and the packing density of the concrete mix: the better the packing, the more water is available to act as lubricant for the solids, and the better the fluidity. Very recently, by Elkem [11] the relation between grading, more particularly: following the modified Andreasen and Andersen (A&A) curve, and SCC is made. It will be demonstrated that the aggregate packing as applied by Su et al. [6] and Su and Miao [7] appears to follow the grading curve of the modified A&A model. Finally, mixes are designed that follow the modified A&A model, but now including all particles (aggregate, filler and cement). Based on this design method, mixes are composed using slag blended cement, limestone powder and gravel, and investigating the role of the three types of sand. It appears that fine sand is a useful component in optimising the PSD, and thereby increasing the stability and flowability of the concrete mix. It is also a major source of reducing the costs of the mix.

## 2. Mix design

The principal consideration of the Chinese Method is that the voids of the aggregate are filled with paste (cement, powder, water). The voids need to be filled with paste so that a workable fresh concrete is attained. Upon the design of SCC it is usually more difficult to achieve satisfactory workability than required strength [6]. The Chinese Method starts with the content of aggregate, which greatly influences the workability: the more aggregate, the less paste and hence, less fluidity. Subsequently, the amount of cement is assessed. This quantity is determined by the required compressive strength and durability of the hardened concrete. This approach corresponds to the Dutch Method of the design of "normal" medium strength concrete. The amount of cement is also determined by the water/cement ratio and durability requirements.

As said, the main consideration of the Chinese Method is that voids present in loose aggregate are filled with paste, and that the packing of the aggregates is minimized. This is achieved by using more sand and less gravel (each about 50%). Here, it will be investigated how this maximum packing can be achieved, and a relation is made with the grading curve of the modified A&A model. The Chinese

Table 1
Properties of materials used

| Material | Type | $\rho$ [kg/m$^3$] | $\rho^l$ [kg/m$^3$] | Blaine [cm$^2$/g] | $S$ [cm$^2$/cm$^3$] |
|---|---|---|---|---|---|
| Cement | CEM III/B 42.5 N LH/HS | 2950 | 1100 | 4700 | 13,865 |
| Filler | Limestone powder | 2740 | 1110 | 4600 | 12,604 |
| Filler | Fly ash | 2250 | 1000 | 3900 | 8775 |
| Coarse sand | Rhine sand 0–4 mm | 2650 | 1631 | – | – |
| Medium sand | Rhine sand 0–2 mm | 2650 | 1619 | – | – |
| Fine sand | Sand 0–1 mm | 2650 | 1511 | – | – |
| Gravel | Rhine gravel 4–16 mm | 2650 | 1604 | – | – |
| Superplasticizer | Glenium 27 (Masterbuilders) | 1045 | | | |

Method makes a distinction between loose packing, and packing after compaction. As SCC is not vibrated, the densest packing cannot be assumed right away.

The void part of loose aggregates generally amounts to about 42–48%. Upon application in SCC, mixing and resulting compaction, the void part is reduced to 32–41%. In the Chinese Method this void reduction is expressed with the help of a Packing Factor (PF). The PF represents the apparent density of aggregate in state of packing in SCC compared with the apparent density of loosely packed aggregate:

$$\mathrm{PF}^{\mathrm{SCC}} = \frac{\text{apparent density aggregate in SCC}}{\text{apparent density loose aggregate}} = \frac{\rho^{\mathrm{d}}}{\rho^{\mathrm{l}}} \qquad (1)$$

If the density of the loosely packed aggregate amounts to 1500 kg/m$^3$ and the density of the aggregate in SCC to 1750 kg/m$^3$, then the PF has a value of 1.17. The PF that can be attained in SCC (PF$^{\mathrm{SCC}}$) will be smaller than the value that can be achieved by vibrating the aggregate. In the Chinese Method the PF is assessed, and multiplied with the loose densities of coarse (gravel) and fine (sand) aggregates.

However, the density of the aggregate mix depends on the sand/gravel ratio, and not solely on those of sand or gravel alone (as are used in both Japanese and Chinese Methods). The void fraction of the compacted aggregate and its apparent (or packing) density are directly related to the aggregate's specific (or particle) density via:

$$\varphi^{\mathrm{d}} = 1 - \frac{\rho_{\mathrm{a}}^{\mathrm{d}}}{\rho_{\mathrm{a}}} \qquad (2)$$

The void fraction and density of the loosely piled aggregate are related via the same equation. To get an indication for the loose and compacted void fraction of the aggregate, an 8 l container was filled with mixes of dry aggregate and the mass of these mixes measured before and after compaction (by vibration) [12]. For three types of sand the densities in combination with gravel has been determined. The densities and other relevant properties of the materials used are summarized in Table 1. In Fig. 2 the particle distribution (PSD) of the materials used is presented (cumulative finer fraction). The PSD of the sands and gravel is determined by sieving, the PSD of cement and limestone powder by laser granulometry. In Fig. 3 the average void fraction is depicted prior to and after compaction of the various sand/gravel mixes. Comparing the loose and compacted void fractions, one can see that by vibrating the void fraction of the loose mix

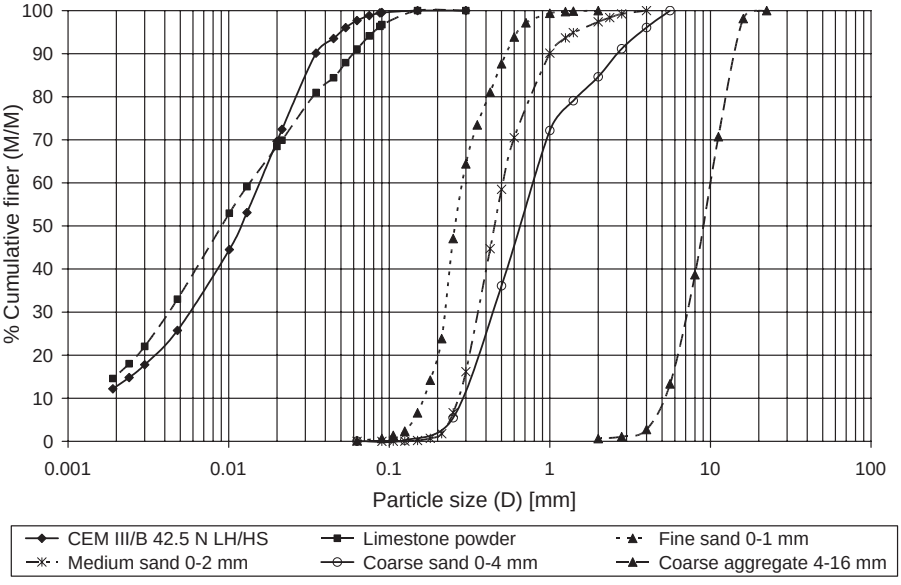


Fig. 2. PSD of aggregates and powders used (cumulative finer mass fraction).

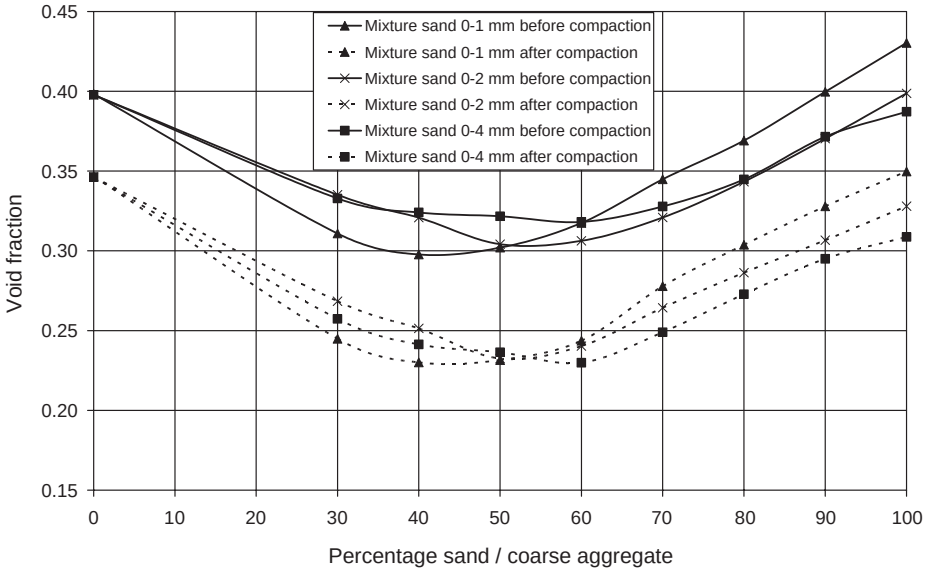


Fig. 3. Void fraction of sand (3 types)/gravel mixes, before and after compaction at various sand contents (m/m) in sand/gravel mixes.

is reduced by a constant factor, about 75–80%. In Section 8 this reduction is compared to the compaction of powders when they are combined with water to form paste.

Furthermore, Fig. 3 reveals that all sand/gravel mixes attain a minimum void fraction with sand/gravel (mass) ratios of 40/60 to 60/40 (both in loose and compacted condition). The coarser the sand, the higher the most favourable sand content (as a smaller volume of the concrete will then comprise paste). Fine sand (0–1 mm) attains a minimum void fraction when its content is 40%, medium sand (0–2 mm) at 50%, and coarse sand (0–4 mm) at 60% in combination with gravel. In loose condition this minimum void fraction amounts to 30%, after compaction to about 23%. In the experimental part later-on attention will be paid to $\varphi^{SCC}$ that can be achieved in fresh SCC. The experiments with sand and gravel reported here give an indication which contents will yield a minimum void fraction.

The mass and volume of the aggregate per m$^3$ of concrete now reads:

$$V_a = \frac{M_a}{\rho_a};\ V_a = \left(1 - \varphi^{SCC}\right)m^3 \tag{3}$$

The second step is the computation of the cement content. The required cement content follows from the desired compressive strength. The Chinese Method assumes a linear relation between the cement content and compressive strength ($f'_{ck}$). Accordingly, the mass and volume of cement follow from:

$$M_c = \frac{f'_{ck}}{x};\ V_c = \frac{M_c}{\rho_c} \tag{4}$$

The value of $x$ appeared to range from 0.11 to 0.14 N/mm$^2$ per kg OPC/m$^3$ concrete [7]. Later, during the experiments, the value of $x$ will also be determined for the slag blended cement used here (Table 1). As Su et al. [6] and Su and Miao [7] used a mix of OPC (200 kg/m$^3$ concrete) and granulated slag, slag blended cement is employed here.

The quantity of water for the cement and the filler (the powders, Fig. 1) is based on the flowability requirement. The water needed for these powders follows from flow spread tests with the Haegermann flow cone, executed analogously to Domone and Wen [13]. Ordinary tap water is used as the mixing water for the present research. For the various water/powder ratios the slump ($d$) and relative slump ($\Gamma_p$) are computed via:

$$d = \frac{d_1 + d_2}{2};\ \Gamma_p = \left(\frac{d}{d_0}\right)^2 - 1 \tag{5}$$

In Fig. 4 the relative slump $\Gamma_p$ is set out against the water/powder mass ratio ($M_w/M_p$) for cement, fly ash and limestone powder. A straight line is fitted and the intersection with the $y$-axis ($\Gamma_p$=0) yields the water content whereby no slump takes place, i.e. the water content that can be retained by the powder. From Fig. 4 for instance follows that for cement flow is possible if $M_w/M_c > 0.33$.

Flowing requires $\Gamma_p > 0$, and when powders are combined, and the water/powder ratio such that $\Gamma_p$ of each powder is equal. The mass and volume of water per m$^3$ of concrete thus becomes:

$$M_w = \left(a_c\Gamma_p + b_c\right)M_c + \left(a_f\Gamma_p + b_f\right)M_f;\ V_w = M_w/\rho_w;\ V_f = M_f/\rho_f \tag{6}$$

The coefficients $a_c$, $b_c$, etc., follow from the fitted lines in Fig. 4, which are crossing each other. This is a consequence of the fact that the relative slump is related to the mass ratio

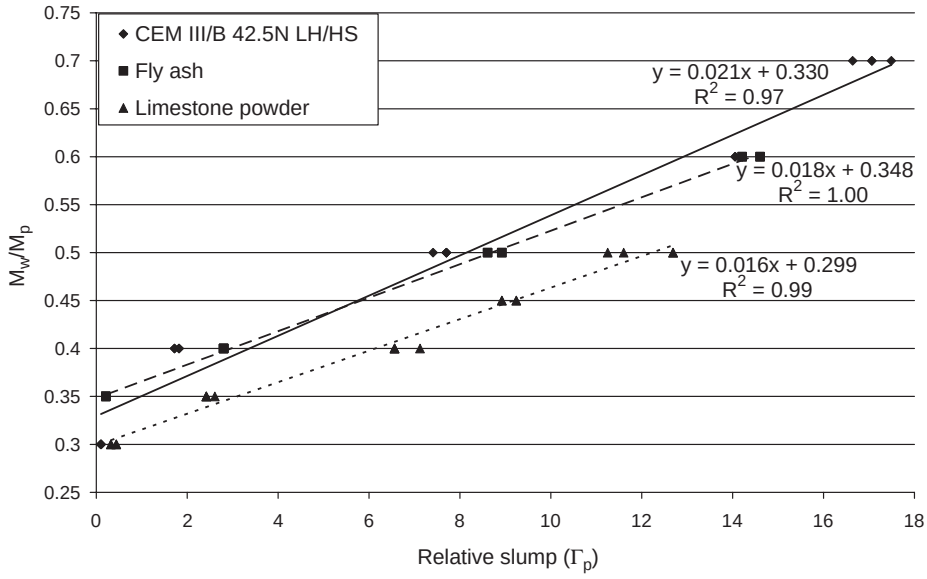


Fig. 4. $M_w/M_p$ versus relative slump for three powders (cement, fly ash, stone powder).

of water and powder, whereas for slurry the volumes of water and solids are relevant. Hence, in Fig. 5 the relative slump is depicted versus the volume ratio of water and powder ($V_w/V_p$), as it is also usual in the Japanese Method. The mass ratio can readily be expressed in the volume ratio by using $M_w/M_c=\rho_w V_w/\rho_c V_c$ for cement, etc. The particle densities from the powders are taken from Table 1, and $\rho_w=1000$ kg/m$^3$. Fig. 5 reveals that when volumes are considered, the three paste lines do not cross anymore. Note that the intersection with the $y$-axis corresponds to $\beta_p$ of the Japanese Method [5,13]. In Section 8 the paste lines are examined in detail and related to some basic physical properties of the powder, such as Blaine value and particle density.

The volume of filler per m$^3$ of concrete now follows as:

$$V_f = 1\ m^3 - V_a - V_c - V_w - V_{SP} - V_{air} \quad (7)$$

The air volume per m$^3$ of concrete, $V_{air}$, is a priori estimated to be 0.015 m$^3$ (=1.5%), this value will be verified later. The solids content of the admixture, superplasticizer, follows from:

$$V_{SP} = \frac{dm_{SP} M_{SP}}{\rho_{SP}} \quad (8)$$

In Eq. (8) $M_{SP}$ is the total mass of superplasticizer (inclusive of water), $dm_{SP}$ is the dry matter and $\rho_{sp}$ the density of the dry matter. For the superplasticizer used (Glenium 27, Masterbuilders) $dm_{SP}=20\%$ and $\rho_{sp}=1045$ kg/m$^3$. Glenium 27, a so-called "3rd generation" superplasticizer, consists of carboxylic

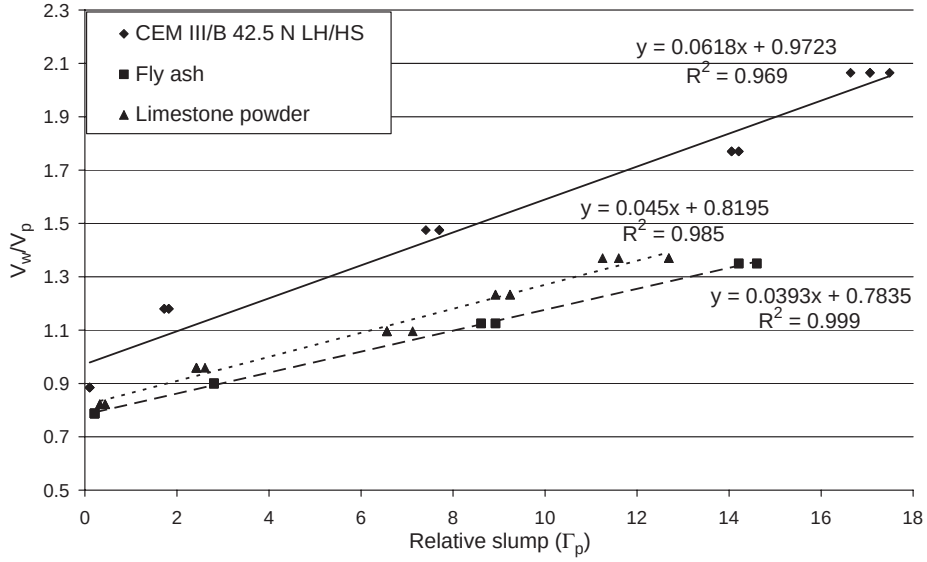


Fig. 5. $V_w/V_p$ versus relative slump for three powders (cement, fly ash, stone powder).

Table 2a
Maximum w/c ratio for each Durability Class (NEN 5950 [14])

| Durability Class | 1 | 2 | 3 | 4 | 5a | 5b | 5c | 5d |
|---|---|---|---|---|---|---|---|---|
| w/c | 0.65 | 0.55 | 0.45 | 0.45 | 0.55 | 0.50 | 0.45 | 0.45 |
| w/c with air entrainment | | | 0.55 | 0.55 | | | | |

ether polymer with lateral chains. The dry matter is related to the total amount of powder by:

$$M_{SP} = n(M_c + M_f) = n(\rho_c V_c + \rho_f V_f) \tag{9}$$

Practical values of n are 0.4–1.7%. The amount of filler follows by combining Eqs. (6)–(9):

$$V_f = \frac{\phi^{SCC} m^3 - V_{air} - \left(1 + a_c \Gamma_p + b_c + dm_{SP} \cdot n \cdot \frac{\rho_c}{\rho_{SP}}\right)}{1 + a_f \Gamma_p + b_f + dm_{SP} \cdot n \cdot \frac{\rho_f}{\rho_{SP}}} \tag{10}$$

The filler volume decreases with the increasing relative slump ($\Gamma_p$). The water/cement ratio follows from:

$$w/c = \frac{M_w}{M_c} = \frac{\rho_w V_w}{\rho_c V_c} = \frac{\rho_w (a_c \Gamma_p + b_c) V_c + \rho_w (a_f \Gamma_p + b_f) V_f}{\rho_c V_c} \tag{11}$$

With increasing $\Gamma_p$ the w/c increases. Also increasing filler volume augments the w/c, as this volume also requires water, whereas the cement content remains the same. According to Dutch Standards, however, the w/c is limited to a maximum value, prescribed by the prevailing Durability Class (Table 2a). In the Japanese Method, $\Gamma_p \approx 0$ is approached as much as possible, in what follows (Sections 4 and 5), for the Chinese Method $\Gamma_p$ ranges from 1 to 2.

Now, the volumes of aggregate, cement, air, superplasticizer, filler and water in the concrete are known. The amount of mixing water follows from Eq. (6), whereby account is taken from the water (free moist) present in aggregate and superplasticizer:

$$M_{w,t} = (a_c \Gamma_p + b_c) M_c + (a_f \Gamma_p + b_f) M_f - (1 - dm_{sp}) \cdot M_{SP} - (1 - dm_a) \cdot M_a \tag{12}$$

In this section, masses and volumes of the concrete ingredients are determined. The solids, aggregate and powders, consist of gravel, sand, filler and cement. In the next section the PSD of each component and the ideal PSD and packing of the entire solids mix will be analysed.

## 3. Packing theory

The Japanese and Chinese Methods do not pay attention to the PSD of the aggregates. It is however known that the viscosity of slurry becomes minimal (at constant water content) when the solids have tighter packing [10]. When particles are better packed (less voids), more water is available to act as a lubricant between the particles. In this section the effect of grading and packing on workability is addressed.

For "normal concrete", most design codes require continuous grading to achieve tight packing. Continuous grading curves range from 250 μm to a maximum particle size (Fuller curve). For modern concretes, such as High Strength Concrete and SCC this Fuller curve is less suited. This curve is applicable to materials with a particle size larger than 500 μm. Applying this grading curve to materials with fine constituents results in mixes that are poor in cement and that are less workable. The Dutch Standard NEN 5950 [14] therefore requires a minimum content of fine materials (<250 μm) in normal concrete (Table 2b). As the content and PSD of fine materials (powder) cannot be determined properly with the Fuller curve, it is less suited for SCC as a large part of the solids consist of powder.

Actually, the packing theory of Fuller and Thompson [15] represents a special case within the more general packing equations derived by Andreasen and Andersen [9]. According to their theory, optimum packing can be achieved when the cumulative PSD obeys the following equation:

$$P(D) = \left(\frac{D}{D_{max}}\right)^q \tag{13}$$

$P$ is the fraction that can pass the sieve with opening $D$, $D_{max}$ is maximum particle size of the mix. The parameter $q$ has a value between 0 and 1, and Andreasen and Andersen [9] found that optimum packing is obtained when $q \approx 0.37$.

The grading by Fuller is obtained when $q = 0.5$. The variable $q$ renders the A&A model suitable for particle sizes smaller than 500 μm. In general, the more powders (<250 μm) in a mix, the smaller the $q$ that best characterizes the PSD of the mix [11]. To validate the hypothesis of tight packing and the application of the A&A model, the PSD of the Chinese Method is analysed. In Fig. 6 the PSD of the aggregates are graphically depicted, based on the sieving data given by Su et al. [6] and Su and Miao [7]. As no sieve information is provided for the powders, it is not possible to depict the PSD down to 1 μm. But the PSD of the entire solid mix is corrected for this powder content, which is known. In Fig. 6 also the grading curves of Fuller and A&A (with $q = 0.3$) are depicted.

Fig. 6 reveals that the Chinese Method seems to follow the grading curve of the A&A theory with $q = 0.3$. With the

Table 2b
Minimum amount of fine material per $m^3$ of concrete (NEN 5950 [14])

| Largest grain size ($D_{max}$) [mm] | Minimum vol. fraction fine material (<250 μm) in concrete |
|---|---|
| 8 | 0.140 |
| 16 | 0.125 |
| 31.5 | 0.115 |

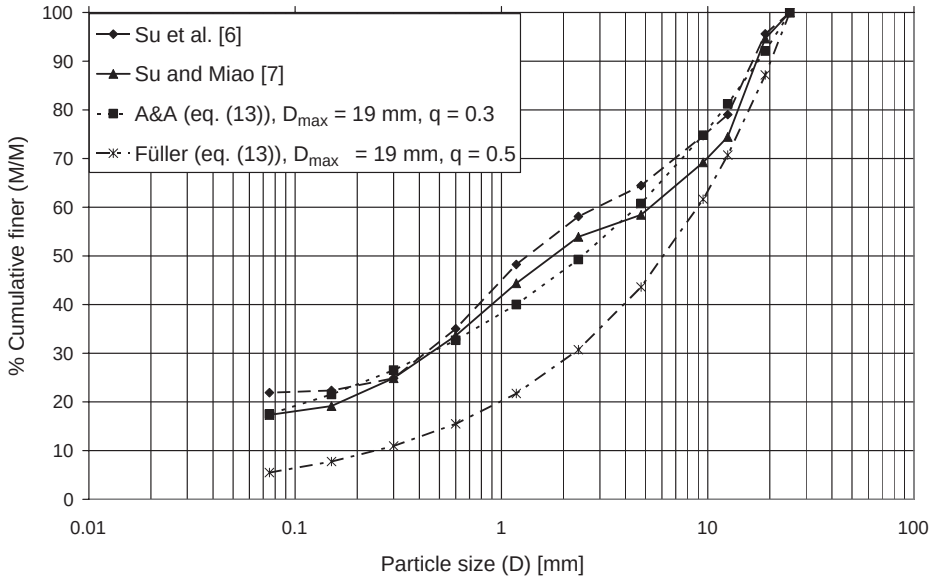


Fig. 6. Analysis of actual PSD of aggregates used by Su et al. [6] and Su and Miao [7].

available ingredients in The Netherlands and their PSD's (Fig. 2), it will be difficult to compose a mix that can approach this A&A curve to the same extent. Fig. 6 confirms that the grading curve of A&A better accounts for powders than the grading curve of Fuller. From the curves in Fig. 6 it furthermore follows that about 20% of the particles are finer than 75 μm, whereas, according to Fuller, only 5.5% are smaller than 75 μm. As the A&A model accounts for powders (<250 μm) better, it is better suited for designing SCC. A continuous grading of all solids (aggregate and powders) will result in a better workability and stability of the concrete mix.

The A&A model prescribes a grading down to a particle diameter of zero. In practice, there will be a minimum diameter in the mix. Accordingly, a modified version of the model is applied that accounts for the minimum particle size in the mix (Funk and Dinger [10]). This modified PSD (cumulative finer fraction) reads:

$$P(D) = \frac{D^q - D_{\min}^q}{D_{\max}^q - D_{\min}^q} \tag{14}$$

whereby $D_{\min}$ is the minimum particle size in the mix. For many years the same equation is also used in mining industry for describing the PSD of crushed rocks [16].

In a 'double-logarithmic' graph, the A&A model results in a straight line, whereas the modified A&A model results in a curve that bends downward when the minimum diameter is approached. In Fig. 7 both curves are given for $q = 0.25$ and $D_{\min} = 0.5$ μm. In the next sections, for the

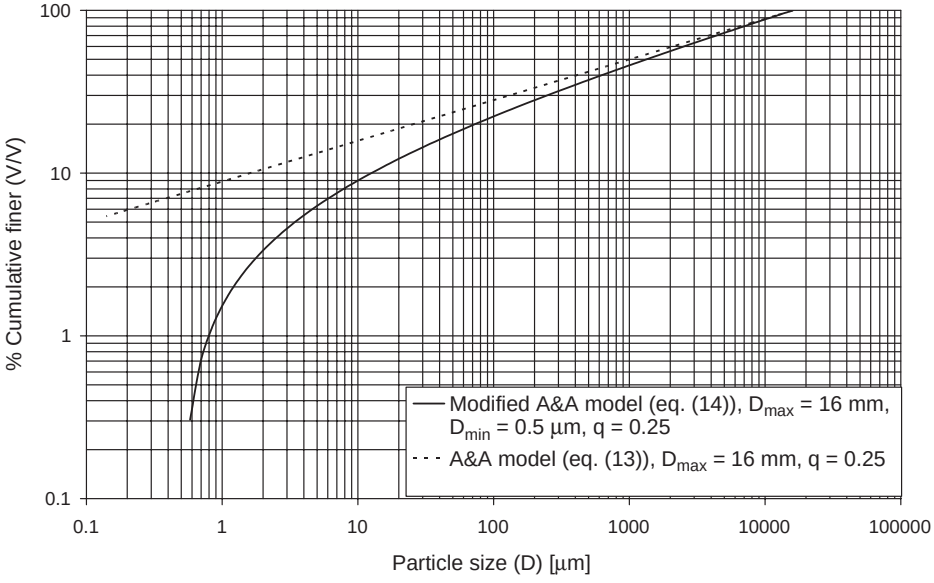


Fig. 7. Cumulative finer volume fraction according to A&A model (Eq. (13)) and modified A&A model (Eq. (14)).

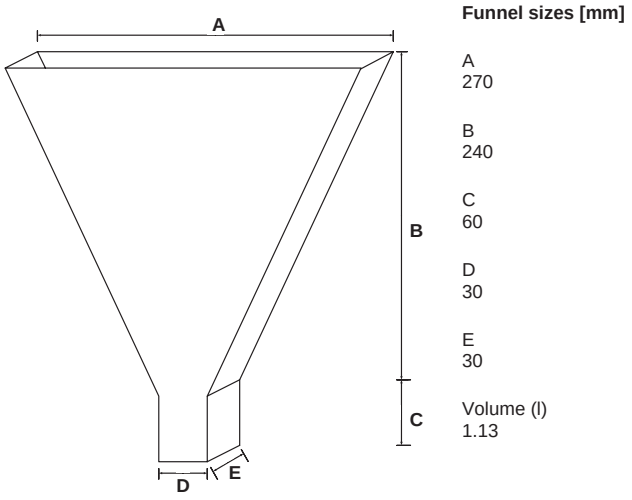


Fig. 8. Sizes of V-funnel used for mortar experiments.

design of the SCC mixes, use will be made of the modified A&A model.

## 4. Mortar experiments

The Chinese Method does not include mortar experiments. In this research they are included as mortars permit a quick and handy scan of preliminary mix designs. For mortar only trial batches of 1.8 l need to be prepared (as gravel is omitted), whereas for concrete a trial batch comprises at least 15 l. The mortars are prepared following the procedure described by the Dutch Precast Concrete Manufacturers Association [17] and is described in detail in Radix [12]. The prepared mortars are evaluated by Slump-flow and V-funnel tests. The Slump-flow test determines the flowability, and the V-funnel test the segregation resistance.

For the Slump-flow test the Haegermann cone is used, which was also used for the powders (Section 2). The slump ($d$) and relative slump of the mortar ($\Gamma_m$) follow from Eq. (5). The sizes of the used V-funnel are depicted in Fig. 8, and the procedure which followed is described in Radix [12].

In practice and in literature different target slumps and V-funnel times are given:

- slump 240–260 mm, funnel time 7–11 s (EFNARC [18]);
- slump 265–315 mm, funnel time 9–10 s. (Ankoné [19]);
- slump 305–325 mm, funnel time 7–9 s. (BFBN [17]);
- slump 250 mm, funnel time 9–11 s. (Walraven et al. [20]).

Following Bos [4], here for mortars the target slump is set at 320 mm and the funnel time at 8 s.

First, a number of experiments with coarse sand (0–4 mm) were carried out. It followed that $n=1.2\%$ (see Eq. (9)) yield satisfactory results [12]. Subsequent experiments with concrete learned that a mortar funnel time of 8 s is actually too long. It appeared that if the mortar funnel time amounts to 5 or 6 s, the funnel time of the concrete meets the target (to be discussed in next section).

The content of coarse sand (0–4 mm) in the mortar can be further modified by applying medium sand (0–2 mm). This introduces finer material in the mix, and it is expected that segregation resistance and workability will benefit. To this end, 40% of the coarse sand is replaced by medium sand. With a lower SP dosage, $n=1.1\%$, now the target funnel time of 5 s is achieved.

Next, fine sand (0–1 mm) is introduced; this fine sand replaces 40% of the coarse sand. The SP dosage can now be reduced even more, with $n=1.0\%$ the required target time is attained.

The mortar experiments are useful for a quick evaluation of designed mixes, and it appears that when the mortar funnel time amounts to 5 or 6 s, the target concrete funnel time will be achieved. It also follows that a better grading of all particles in the mix reduces the required SP dosage. In the following section the experimental evaluation of fresh concrete is addressed.

## 5. Fresh concrete experiments

The three mixes that have been designed in the previous section will be examined in detail here, whereby the gravel is now also included. Details on the preparation procedure of the concrete mixes can be found in Radix [12].

In The Netherlands, basic evaluation tests for SCC have been developed which can also be executed on site. A number of these test are described in CUR [21] and BMC [22], being in line with current international methods [18]. In Table 3 the various test methods are summarized which are used to measure the workability of SCC, taken from EFNARC [18].

The consistence of the concrete mix is assessed by the slump and the time needed to attain a slump of 50 cm ($T_{50}$), using the Abrams cone. The slump ($d$) is determined with Eq. (5), whereby $d_1$ and $d_2$ are the maximum diameters, rounded off at 5 mm. The final slump should range from 630 mm to 800 mm and the target flow time, $T_{50}$, amounts to 2 to 5 s [21]. A visual inspection also gives an indication of the degree of segregation. The test is executed according to BMC [22] and CUR [21].

Table 3
List of test methods for workability properties of SCC (EFNARC [18])

| Property | Test method |
|---|---|
| Filling ability | Slump flow |
| | Slump flow ($T_{50}$) |
| | V-funnel |
| Passing ability | J-ring |
| Segregation resistance | V-funnel ($T_5$) |

With the help of a V-funnel, the flowing time is determined two times ($T_1$ and $T_2$), the arithmetic mean being the mean flow time ($\bar{T}$). This mean time gives an indication of the viscosity and filling time of the mix. The sizes of the funnel depend on the maximum aggregate size (Table 4), here 16 mm. The V-funnel test is executed according to the guidelines given by CUR [21]. According to this, $\bar{T}$ should range from 5 to 15 s, BMC [22] prescribes $\bar{T}$ to lie between 5 and 15 s. The segregation resistance is determined by measuring the flow out time 5 min after the funnel has been filled ($T_5$). The stability time ($T_s$) is defined as:

$$T_s = T_5 - \bar{T} \tag{15}$$

whereby $T_s = 0$ if $T_5 < \bar{T}$. BMC [22] prescribes that $T_s$ should be smaller than 3 s.

The passing ability of the mixes is tested with the help of the J-ring. The J-ring is an open rectangular steel ring, thickness 25 mm, inner diameter 260 mm and outer diameter 324 mm. Vertical holes are drilled (72), which can accept vertical bars that can be spaced at different intervals. The diameter of the bars is 16 mm, and their height 100 mm. The number and spacing of the bars is in accordance with reinforcement considerations: when the largest aggregate size is below 12 mm, 24 bars are used, below 20 mm, 18 bars, and below 32 mm, 12 bars [21]. As the largest grain size is 16 mm, 18 bars are used. This implies that the gap between the bars is about 37 mm, corresponding to about 2.3 maximum grain sizes.

The J-ring is placed in conjunction with the Abrams cone, which is placed centrally inside the J-ring. After the concrete has flown out freely, the extent of blocking is measured [21]. The blocking step ($B$) is computed with:

$$B = 2(h_{in} - h_{ex}) - (h_c - h_{in}) \tag{16}$$

whereby $h_c$, $h_{in}$ are $h_{ex}$ the height of the mix in the centre, just inside the bars and just outside the bars, respectively, measured at four locations and averaged. The blocking step should be smaller than 15 mm [21]. The concrete is also inspected visually to evaluate segregation and blocking.

It is known that the performance of superplasticizers decays with time. In particular, for the ready-mixed concrete industry, the workability should not reduce too much with time and a constant (or minimum preserved) workability is of major importance. To assess the preservation of the workability, the Slump-flow and J-ring tests are also measured at 15, 30, 45, 60, 90 and 120 min after preparation of the mixes. Ready-mixed concrete is slowly stirred upon transport in the truck-mixer. To simulate this truck mixing, the concrete was also stirred; after each 4 min of rest, the concrete was rotated for 1 min in the mixer. Finally, also the air content of the fresh concrete is measured. The design method assumes an air content of 1.5% (volume), see Section 2.

Table 5 contains the final mix proportions of the developed SCC, based on the mortar and concrete tests. The table reveals that the sand content is high, and that all three mixes have an aggregate void fraction ($\phi^{SCC}$) of 36%. Furthermore, the total powder content (cement plus limestone powder) amounts to 473 kg/m$^3$ to 499 kg/m$^3$ only. Table 6 reveals that all three mixes meet the set requirements discussed above. Figs. 9 and 10 depict the slump flow and blocking step with time, respectively. Fig. 9 shows that the slump flow decreases linearly with time, after an increase during the first 15 min. A possible explanation for this increase is that the SP needs some time to become active. In particular, the slump loss of Mix A is most pronounced in time. On the other hand, Mixes B and C follow a similar line and after 2 h they still meet the minimum slump flow of 650 mm.

Fig. 10 reveals that after 45 min Mix A exceeds the maximum blocking step of 15 mm. After 60 min Mix A clearly exhibits substantial blocking. Mix B is performing better than Mix A, but after 45 min it does not meet the

Table 4
Sizes V-funnel (see Fig. 8)

| Type | Grading | | | |
|---|---|---|---|---|
| | 0–4 | 0–8 | 0–16 | 0–32 |
| A | 270 | 390 | 515 | 600 |
| B | 240 | 350 | 450 | 515 |
| C | 60 | 105 | 150 | 195 |
| D | 30 | 40 | 65 | 85 |
| E | 30 | 40 | 75 | 95 |
| Vol. (l) | 1.13 | 3.27 | 10.51 | 18.30 |

Here the sizes pertaining to grading 0–16 are used (shaded area).

Table 5
Dosages of developed mixes

| Material | Mix A [kg/m$^3$] | Mix B [kg/m$^3$] | Mix C [kg/m$^3$] |
|---|---|---|---|
| Cement | 310 | 315 | 320 |
| Limestone powder | 189 | 164 | 153 |
| Sand 0–1 mm | – | – | 388 |
| Sand 0–2 mm | – | 306 | – |
| Sand 0–4 mm | 1018 | 719 | 628 |
| Gravel 4–16 mm | 667 | 673 | 687 |
| Water | 170 | 173 | 174 |
| Superplasticizer | 6.0 | 5.51 | 5.21 |
| Water/cement ratio | 0.55 | 0.55 | 0.55 |
| Water/powder ratio | 0.34 | 0.36 | 0.37 |

Table 6
Results of fresh concrete tests

| Result | Mix A | Mix B | Mix C |
|---|---|---|---|
| Slump [mm] | 720 | 745 | 730 |
| Slump flow time $T_{50}$ [s] | 3 | 3 | 3 |
| Blocking step [mm] | 14.50 | 4 | 12.50 |
| Mean funnel time [s] | 12 | 11.5 | 12 |
| Funnel time after 5 min $T_5$ [s] | 15 | 14 | 15 |
| Air content [V/V %] | 2.6 | 1.7 | 2.5 |
| Density [kg/m$^3$] | 2220 | 2200 | 2200 |

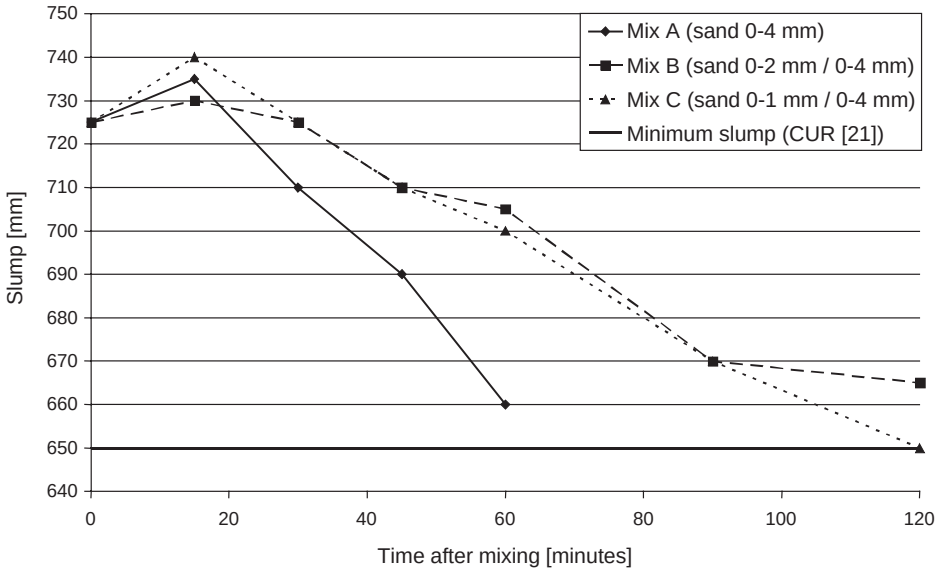


Fig. 9. Slump flow reduction with time.

maximum allowable blocking step either. Mix C meets the requirements during 60 min and exceeds the maximum blocking step only slightly. It should be noted that the blocking of Mixes B and C are very minor, only a slight difference in height is noticeable across the J-ring. The concrete still flows easily along the bars and does not show any sign of segregation. Actually, a reading off error from about 1 mm will already result in a blocking step that is too large. The maximum value set by CUR [21] is quite severe, and is only realistic when the mix height can be measured with an accuracy of 0.1 mm (e.g. with laser). That is the reason that in Germany the difference in Slump-flow with and without J-ring is considered, whereby the difference should be smaller than 50 mm [23]. This difference is easier to measure, and all three mixes meet this requirement. The high retention of filling and passing abilities is most probably owed to the type of plasticizer used. Hanehara and Yamada [24] also observed a longer workability when using a polycarboxylate type admixture.

Table 6 also contains the measured air content and density of the concrete. The air content is higher than 1.5% as assumed during the mix computations. As possible explanation is that the concrete did not have enough time to de-air (5 min) after filling the air-pressure container. But all values are well within the maximum air content of 3% (NEN 5962 [25]). The densities of all three mixes are close. Mix A possesses a slightly higher density as it

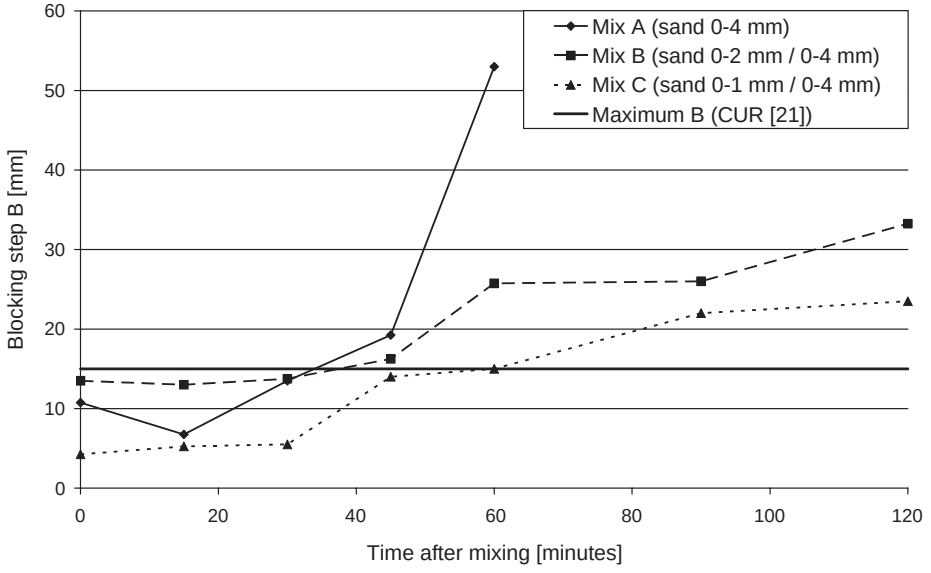


Fig. 10. Blocking step increase with time.

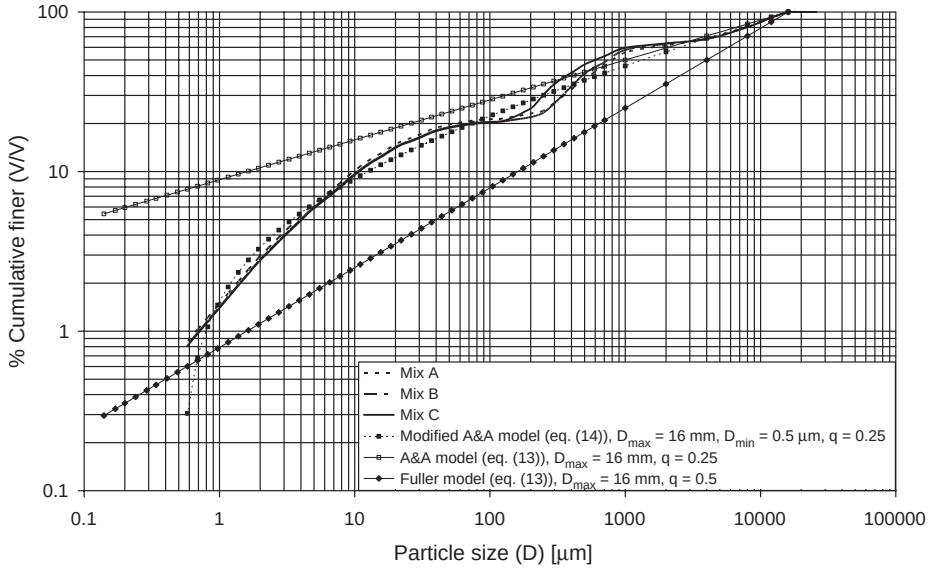


Fig. 11. Cumulative finer mass fraction of Mixes A, B and C in double-logarithmic graph.

contains more powder (Table 5). Mixes B and C have the same density, although Mix C contains less powder than Mix B. But Mix C contains 5 kg/m$^3$ cement more, which has a higher specific density than all other constituents (Tables 1, 5 and 6).

## 6. Grading

In Figs. 11 and 12 the PSD (cumulative finer) of the three mixes are given comprising all solids. In the single-logarithmic graph the grading of the coarse material can be read off clearly. By presenting the PSD also in a double-logarithmic graph, possible deviations in the grading of the fine material (<250 µm) become clear. In both figures also the curves following the A&A grading, the modified A&A grading and the Fuller grading are included.

Figs. 11 and 12 readily reveal that the PSD of the three mixes does not follow the Fuller curve, which is used for "normal" concrete. The designed three mixes follow as much as possible the PSD from the modified A&A grading (with $q=0.25$), as recommended by [11]. However, the PSD from the three mixes cannot follow the modified A&A curve perfectly, as the PSDs of the constituents used are S-shaped (Fig. 2). Especially, between 100 µm and 4 mm one can see a disturbance, which can be explained by the fact that in this particle range the sand contributes significantly to the PSD. The S-shaped pattern corresponds

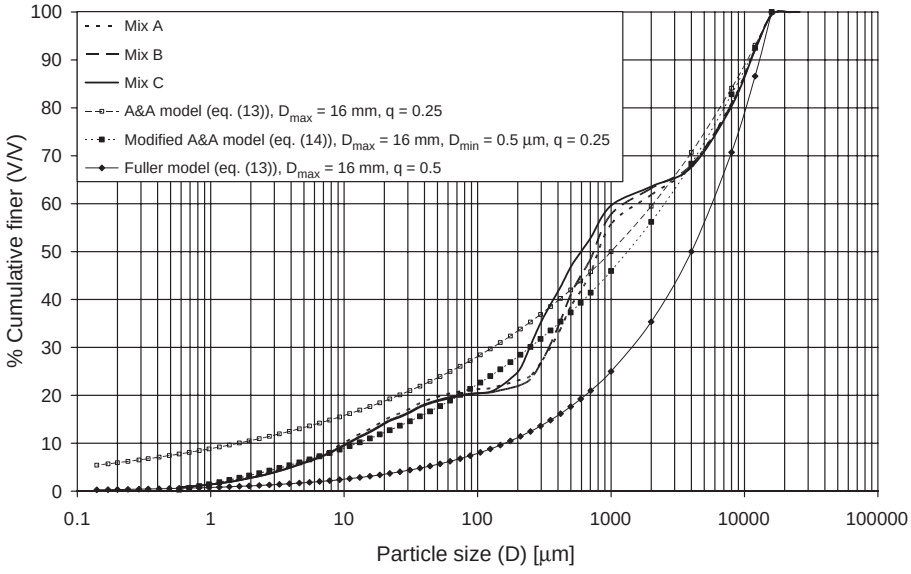


Fig. 12. Cumulative finer mass fraction of Mixes A, B and C in single-logarithmic graph.

to the pattern of the sand (Fig. 2). In order to avoid this deviation, more constituents with overlap in their particle sizes should be used. One can think on the application of sand 2–4 mm and gravel 4–8 mm.

It is expected that a grading that more closely follows the modified A&A curve will result in a mix with a better workability and stability. The three concrete mixes revealed that indeed Mix C exhibited a better resistance to segregation and workability. The required amount of SP in this mix is also lower than in the two other mixes, whereas their slump flows and funnel times are almost equal. The addition of fine sand (0–1 mm) has improved the flowing properties of the mix, so that the amount of powders and SP can be reduced.

Using the modified A&A grading curve, the part of fine materials (<250 μm) is about three times higher than with the application of the Fuller curve. Table 7 lists the amount of fine materials in the three mixes. Table 7 shows that Mix C contains much more fine material than Mixes A and B, and that the quantity of the stone powder is least in Mix C. Hence, by application of fine sand (0–1 mm) it is possible to increase the amount of fine materials, while at the same time reducing the quantity of cement and filler. The volume of fine material in Mix C amounts to about 0.245 $m^3$ per $m^3$ of concrete, which is about two times the minimum amount prescribed by NEN 5950 [14] for concrete with a maximum particle size of 16 mm (Table 2b). This reduction of powders and superplasticizer in case of fine sand application can also be explained by comparing the PSDs of the three mixes. The PSD of Mix C follows best the modified A&A curve, especially between 100 μm and 1 mm (Figs. 11 and 12).

Considering Tables 1 and 5, it follows that all solids (cement, limestone powder and aggregate) take about 81% of the volume of all mixes, i.e. the void fraction amounts about 19%. It is interesting to compare this value with the void fraction of an ideal mix that obeys Eq. (14), which reads [26]:

$$\varphi = \varphi_1 \left(\frac{D_{\min}}{D_{\max}}\right)^{\frac{(1-\varphi_1)\beta}{(1+q^2)}} \tag{17}$$

This equation contains the void fraction of the single-sized particles ($\varphi_1$) and a parameter ($\beta$), which are both governed by the particle shape and method of packing (loose, close) only. From [9,26] it follows that for the irregular particles considered here, $\varphi_1=0.52$ and $\beta=0.16$ (loose), and $\varphi_1=0.46$ and $\beta=0.39$ (close). Furthermore, substituting $D_{\min}=0.5$ μm, $D_{\max}=16$ mm and $q=0.25$, yields $\varphi=25\%$ and $\varphi=6\%$ for loose and close random packing, respectively. Hence, the void fraction of Mixes A, B and C (19%) are situated between these aforementioned two extremes.

The concrete mix tests yield the conclusion that the PSDs and the content of fine materials (<250 μm) greatly influence the stability and workability of the mix. The application of fine sand helps to optimise both content and PSD in the fine particle range, so that the amount of required SP can be reduced. This application of fine sand also reduces the ingredient costs of the mix. Fine sand is relatively cheap; it is cheaper than the two other sands and than gravel, and replaces the most expensive constituents: cement and stone powder (the powders). Furthermore, composing a mix with a PSD that closely follows the modified A&A model reduces another expensive ingredient, namely the SP. It could be expected that if one would optimise the PSD down in the nanometre range, the workability and stability could be maintained while further reducing the necessary SP content. In the next section the tests on the hardened concrete are reported.

Table 7
Amount of fine material (<250 μm) per $m^3$ of concrete

| | Mix A | Mix B | Mix C |
|---|---|---|---|
| Volume fraction fine material (<250 μm) | 0.195 | 0.189 | 0.245 |
| Mass of cement [kg/$m^3$] | 310 | 315 | 320 |
| Mass of stone powder [kg/$m^3$] | 189 | 164 | 153 |
| Part of sand 0–1 mm smaller than 250 μm [kg/$m^3$] | – | – | 180 |
| Part of sand 0–2 mm smaller than 250 μm [kg/$m^3$] | – | 20 | – |
| Part of sand 0–4 mm smaller than 250 μm [kg/$m^3$] | 55 | 39 | 34 |
| Total mass of fine material ($D$<250 μm) [kg/$m^3$] | 554 | 538 | 687 |

## 7. Hardened concrete experiments

The three mixes have been poured in standard cubes of $150\times150\times150$ $mm^3$, cured sealed during the first day, demoulded, and subsequently cured for 27 days submersed in a water basin. In total, 138 cubes have been produced which are tested physically and mechanically. Of each mix, 46 cubes have been produced, 44 for testing, and 2 as reserve. Since the concrete mixer in the laboratory has a limited capacity (25 l), each mix is made in 7 batches: 6 batches of 25 l and 1 batch of 20 l, yielding a total of 170 l for each mix.

The density of the hardened concrete is determined by measuring the weight of a cube in the air and underwater, according to standard NEN 5967 [27]. The density is computed by

$$\rho_{\text{cube}} = \rho_{\text{w}} \frac{M_{\text{cube}}^{\text{air}}}{M_{\text{cube}}^{\text{air}} - M_{\text{cube}}^{\text{water}}} \tag{18}$$

Table 8
Apparent density of hardened concrete

| | Mix A | Mix B | Mix C |
|---|---|---|---|
| Mean cube density [kg/m$^3$] | 2370 | 2360 | 2350 |
| Standard deviation [kg/m$^3$] | 33.3 | 13.0 | 7.5 |
| Coefficient of variation [%] | 1.4 | 0.6 | 0.3 |

where $M_{\text{cube}}^{\text{air}}$ and $M_{\text{cube}}^{\text{water}}$ are the weights of the concrete cube in air and water, respectively. The mean values of all cubes are listed in Table 8. In this table also the two statistical parameters, standard deviation ($s$) and variation coefficient (VC), are given. The standard deviation is computed with:

$$s = \sqrt{\frac{\sum(y_i - \bar{y})^2}{m-1}} \tag{19}$$

where $y_i$ is each measured value, $\bar{y}$ their arithmetic mean value, and m the number of measured values. The coefficient of variation is computed by

$$\text{CV} = \frac{s}{\bar{y}} \tag{20}$$

The $s$ and CV listed in Table 8 show that all batches have resulted in concrete with almost constant density (the difference is less than 1%), so that all batches are very homogeneous and identical.

The compressive strength ($f_c$) of each cube is measured according to standard NEN 5968 [28]. At ages of 1, 3, 7 and 28 days, 5 cubes per mix are tested and the resulting mean values are listed in Table 9a–d and depicted in Fig. 13a.

Mix C has the highest compressive strength; application of the fine sand (0–1 mm) seems to contribute to the strength, most likely by a better packing of the particles. Though Mix B contains medium sand (0–2 mm) and more cement than Mix A, it has a lower compressive strength than Mix A.

To classify the mixes, the characteristic compressive strength ($f'_{ck}$), being the strength that is statistically attained by 95% of the material, is determined. It follows from the mean value ($\bar{y}$), the standard deviation ($s$) and the eccentricity ratio ($e$) as:

$$f'_{ck} \leq \bar{y} - e{\cdot}s \tag{21}$$

The value of $e$ depends on the number of tested cubes (here: 5). In Table 10 the values of $e$ are listed assuming a normal (Gaussian) distribution, here $e=2.37$. In Table 9d the characteristic 28 days strength is included, indicating that the three mixes can be classified as C35/45 (former B45).

In Section 3 it was discussed that Su et al. [6] and Su and Miao [7] used a parameter $x$ to describe the strength of concrete as a function of the cement content (Eq. (4)). To assess the value of $x$ for the cement used here, the characteristic compressive strength (Table 9d) is divided by the cement content of the mix (Table 5) and included in Table 9d. The values found for slag cement CEM III/B 42.5 N LH/HS used here, around 0.15 N/mm$^2$, are higher than the values of Type I Portland Cement, 0.11 to 0.14 N/mm$^2$, reported by Su et al. [6] and Su and Miao [7].

Next, the tensile strength is measured using the indirect splitting test, according to standard NEN 5969 [29]. Two plywood strips (thickness 3 mm, width 15 mm and length 160 mm) are used as bearing strips. At ages of 1, 3, 7 and 28 days, 5 cubes per mix are tested, and the resulting mean values are listed in Table 11a–d and depicted in Fig. 13b. The tensile strength follows from:

$$f_t = \frac{2F}{\pi z^2} \tag{22}$$

where $F$ is the applied yield force and z the side of the cube (z=150 mm). Likewise the compressive strength (Table 9a–d), Mix C also has the highest tensile strength. The tensile strength is related to the compressive strength. For "normal concrete" the 28 days (splitting) tensile strength ($f_t$) can be computed from the compressive strength ($f_c$) by NEN 6722 [30] as:

$$f_t = 1 \text{ N/mm}^2 + 0.05 f_c \tag{23}$$

The measured tensile and compressive strengths of the 3 mixes are depicted in Fig. 14, at an age of 28 days. In this figure also Eq. (23) is included. The experimental

Table 9
Compressive strength (in N/mm$^2$) after 1 day (a), 3 days (b), 7 days (c) and 28 days (d) curing

| | Mix A | Mix B | Mix C |
|---|---|---|---|
| *a)* | | | |
| Mean compressive strength [N/mm$^2$] | 5.7 | 3.9 | 5.9 |
| Standard deviation [N/mm$^2$] | 0.1 | 0.7 | 0.1 |
| Coefficient of variation [%] | 1.8 | 17.9 | 1.7 |
| *b)* | | | |
| Mean compressive strength [N/mm$^2$] | 17.2 | 16.9 | 18.4 |
| Standard deviation [N/mm$^2$] | 0.3 | 0.6 | 0.2 |
| Coefficient of variation [%] | 1.7 | 3.6 | 1.1 |
| *c)* | | | |
| Mean compressive strength [N/mm$^2$] | 31.2 | 28.3 | 34.0 |
| Standard deviation [N/mm$^2$] | 1.8 | 0.8 | 1.0 |
| Coefficient of variation [%] | 5.8 | 2.8 | 2.9 |
| *d)* | | | |
| Mean compressive strength [N/mm$^2$] | 51.2 | 50.7 | 53.6 |
| Standard deviation [N/mm$^2$] | 1.5 | 1.7 | 1.8 |
| Coefficient of variation [%] | 2.9 | 3.4 | 3.4 |
| Characteristic compressive strength [N/mm$^2$] | 47.6 | 46.7 | 49.3 |
| $x$ [N/mm$^2$ per kg cement/m$^3$ concrete] | 0.154 | 0.148 | 0.154 |

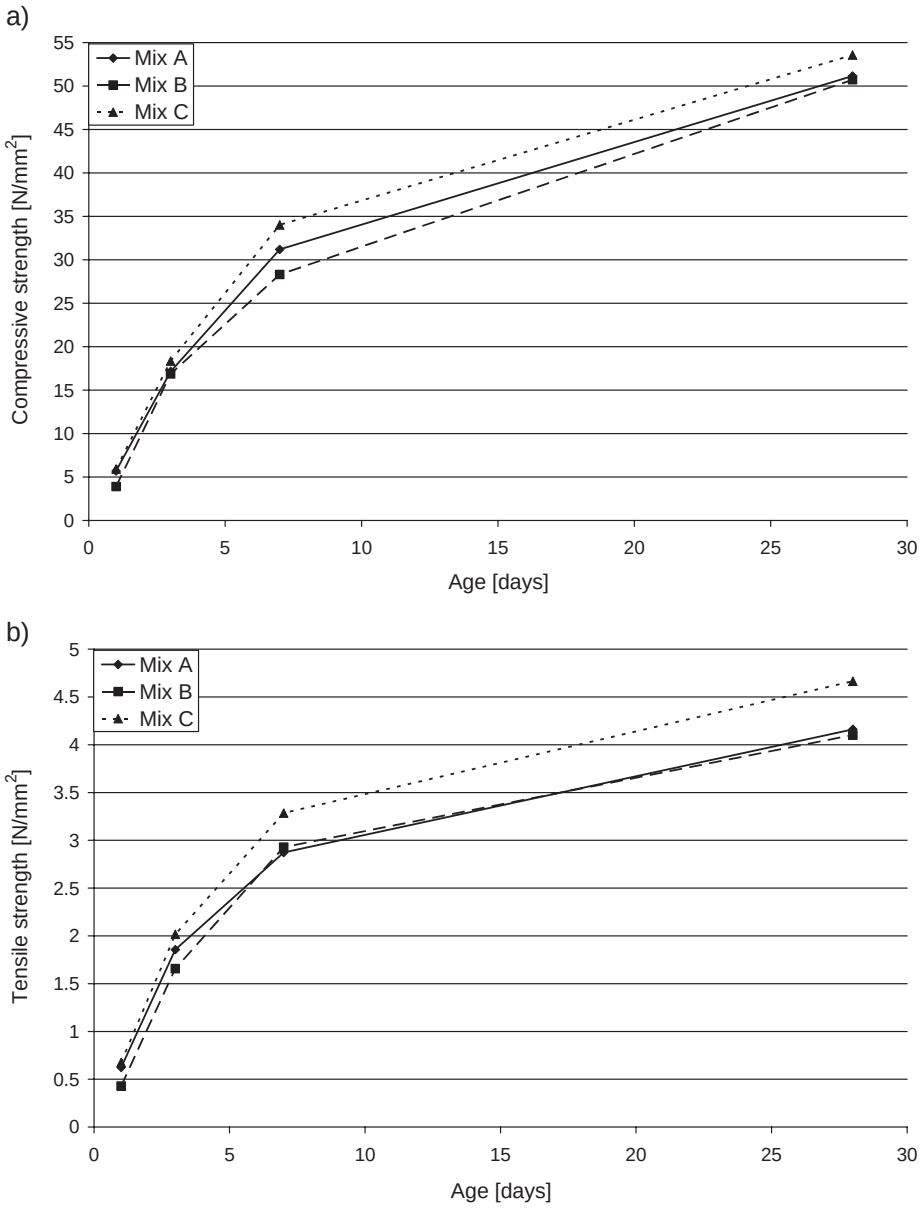


Fig. 13. a) Compressive strength versus age. b) Tensile strength versus age.

results show that the SCC mixes perform better than the empirical correlation (Eq. (23)). This is in line with CUR [21], where it was concluded that the tensile strength of SCC is systematically higher than that of "normal concrete".

Subsequently, the durability of the mixes is investigated by measuring the intrusion of water, by absorption and by pressure at an age of 28 days. The intrusion of water is measured by exposing one face of the cube to water pressure of 5 bars (0.5 MPa), according to standard NEN-EN 12390-8 [31]. After 72 h the cubes are removed from the test rig, and split perpendicularly with respect to the tested face following NEN 5969 [29]. The location of the waterfront, at both halves, can be observed visually and the distance from the cube side measured (Fig. 15). For each mix, two cubes are tested accordingly. In Table 12 the results are listed.

Table 10
Eccentricity factor versus number of tests

| Number of specimen | 12 | 11 | 10 | 9 | 8 | 7 | 6 | 5 | 4 | 3 | 2 |
|---|---|---|---|---|---|---|---|---|---|---|---|
| Eccentricity factor | 1.53 | 1.60 | 1.68 | 1.77 | 1.87 | 2.00 | 2.16 | 2.37 | 2.65 | 3.06 | 3.75 |

The results indicate that the addition of fine sand (0–1 mm) and medium sand (0–2 mm) have a beneficial effect on water resistance. Mix B is having slightly less water intrusion that Mix A, but Mix C clearly has a much lower

Table 11
Tensile strength (in N/mm$^2$) after 1 day (a), 3 days (b), 7 days (c) and 28 days (d) curing

| | Mix A | Mix B | Mix C |
|---|---|---|---|
| *a)* | | | |
| Mean tensile strength [N/mm$^2$] | 0.6 | 0.4 | 0.7 |
| Standard deviation [N/mm$^2$] | 0.02 | 0.12 | 0.01 |
| Coefficient of variation [%] | 3.3 | 30.0 | 1.4 |
| *b)* | | | |
| Mean tensile strength [N/mm$^2$] | 1.9 | 1.7 | 2.0 |
| Standard deviation [N/mm$^2$] | 0.09 | 0.14 | 0.08 |
| Coefficient of variation [%] | 4.7 | 8.2 | 4.0 |
| *c)* | | | |
| Mean tensile strength [N/mm$^2$] | 2.9 | 2.9 | 3.3 |
| Standard deviation [N/mm$^2$] | 0.14 | 0.10 | 0.16 |
| Coefficient of variation [%] | 4.8 | 3.4 | 4.8 |
| *d)* | | | |
| Mean tensile strength [N/mm$^2$] | 4.2 | 4.1 | 4.7 |
| Standard deviation [N/mm$^2$] | 0.27 | 0.27 | 0.20 |
| Coefficient of variation [%] | 6.4 | 6.6 | 4.3 |

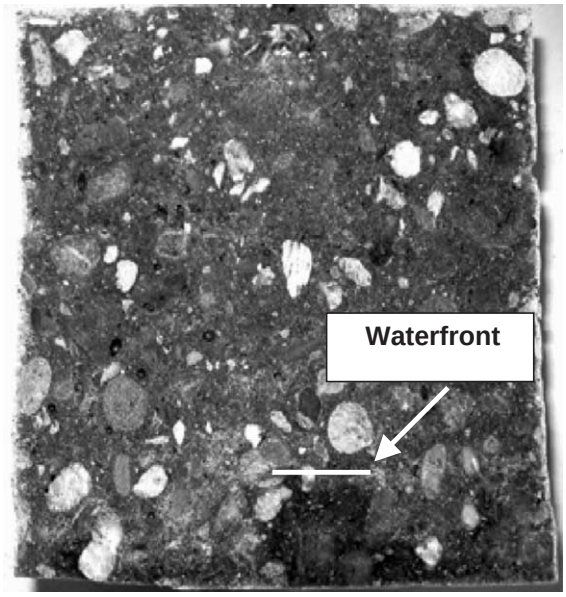


Fig. 15. Photo of water intrusion in one half of the cube.

permeability than both other mixes. Concrete with less than 50 mm intrusion is regarded as impermeable [23]. All three mixes meet this requirement and can be classified as impermeable.

Next, the capillary absorption is measured, analogous to Audenaert et al. [32] and Zhu and Bartos [33]. Prior to the experiment, the cubes (of age 28 days) were dried in an oven at 105±5 °C during 48 h, and cooled down during 24 h at room temperature. Then, the cubes were placed on bars with a diameter of 10 mm, so that the water level is 5±1 mm above the lower horizontal face of the cube. For each mix, two cubes have been tested. The mass increase of each cube is measured after 0.25, 0.5, 1, 3, 6, 24, 72 and 168 h (Fig. 16). Furthermore, the height of the capillary rise is measured on the 4 vertical side faces (in the centre of the side) of each cube; the mean values of each cube, H, are given in Fig. 17.

There is a linear relation between the capillary rise and the square root of time [32,33]:

$$H = H_0 + \mathrm{SI}T^{0.5} \tag{24}$$

In this equation is $H$ the height of the capillary rise, $H_0$ the intersection with the $y$-axis [mm], SI the sorption index [mm/h$^{0.5}$] and $T$ the time (h). The SI is a measure for the uptake of water by a concrete surface exposed to

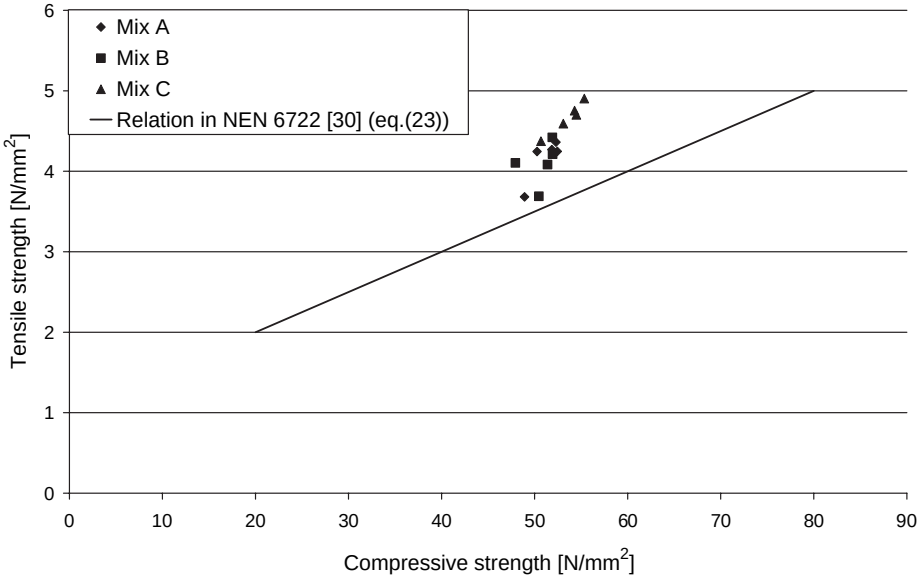


Fig. 14. Tensile strength versus compressive strength (28 days).

Table 12
Water intrusion and permeability (28 days)

| Specimen | Intrusion depth [mm] | | |
|---|---|---|---|
| | Side 1 | Side 2 | Mean |
| Mix A, cube 1 | 30 | 26 | 28 |
| Mix A, cube 2 | 30 | 24 | 27 |
| Mix B, cube 1 | 17 | 21 | 19 |
| Mix B, cube 2 | 21 | 26 | 23.5 |
| Mix C, cube 1 | 8 | 6 | 7 |
| Mix C, cube 2 | 10 | 7 | 8.5 |

rain for instance. In Audenaert et al. [32] it can be found that SI should be smaller than 3 mm/h$^{0.5}$. Using linear regression, the SI is derived from the data in Fig. 17, and listed in Table 13, including the regression coefficient of the fit. One can see that now Mix C is having the highest value, indicating that the fine sand is favourable for capillary suction. But Table 13 also reveals that all mixes have an SI that is well below 3 mm/h$^{0.5}$, so that this durability criterion is met.

## 8. Analysis of powder (paste) and aggregate (vibration) experiments

In this section the aggregate compaction and paste flow spread tests from Section 2 will be analysed in detail. A relation will be derived between the amount of water that can be retained and the void fraction of the powder. Furthermore, a relation will be derived between the slope of the paste line, and the internal specific surface area of the powder. Based on both powder and aggregate data, a general relation is derived that describes the reduction in void fraction upon compaction.

Fig. 5 shows the relative slump, a measure for the flowability, and the ratio of water and powder volume. To interpret this data, two hypotheses will be put forward and validated. First, when sufficient water is present for flow, so $V_w/V_p > \beta_p$, the relative slump depends on the specific surface area of the powder. This is motivated by the concept that water in surplus of $V_p\beta_p$ is able to lubricate the particles. The thickness of this water film, which governs flowability and slump, depends on the internal specific surface area of the paste. Second, it is assumed that the paste will flow when $\Gamma_p > 0$, so there is sufficient water to fill the voids of the powder.

The fitted paste lines of the powders: cement, fly ash and stone powder in Fig. 5, are of the form:

$$V_w = (\alpha_p \Gamma_p + \beta_p) V_p \tag{25}$$

The fitted coefficients $\alpha_p$ and $\beta_p$ are listed in Table 14. To verify the first hypotheses, the deformation coefficient $\alpha_p$ is divided by specific surface area $S$, i.e. the Blaine surface per volume of powder. The specific surface areas of the three powders are listed in Tables 1 and 14, and follow from Blaine multiplied by the particle density. From the limited amount of data, one might draw the conclusion that the larger the internal surface, the larger the deformation coefficient (the more water is required to attain a certain relative slump, see Fig. 5). Accordingly, a linear relation is invoked:

$$\alpha_p = \delta \cdot \text{Blaine} \cdot \rho_p = \delta \cdot S \tag{26}$$

Substituting $\alpha_p$ and $S$ from the three powders yields that $\delta$ ranges from $3.570 \times 10^{-6}$ cm to $4.478 \times 10^{-6}$ cm

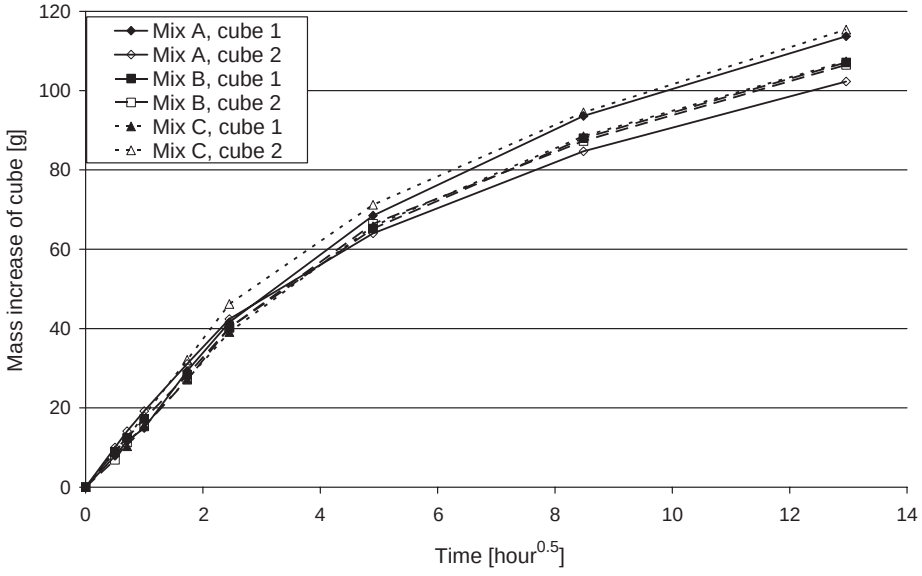


Fig. 16. Mass increase of concrete cube by capillary suction with time.

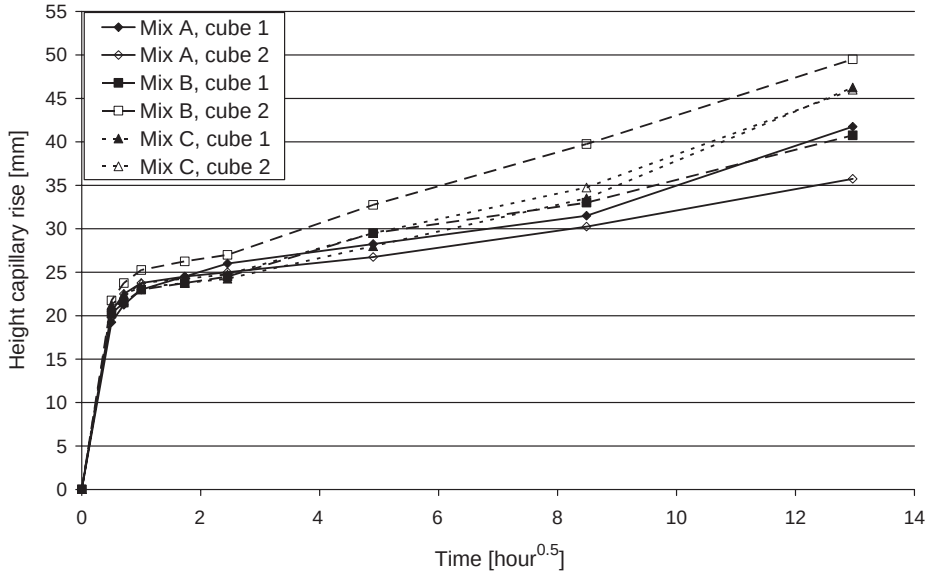


Fig. 17. Mean capillary rise of each cube with time.

(Table 14), with $\delta = 4.132 \times 10^{-6}$ cm being a mean value that matches all three computed values of δ (within 13.6%). In Fig. 18a the experimental $\alpha_p$ and S and Eq. (26) with $\delta = 41.32$ nm are set out. Furthermore, comparable data taken from Domone and Wen [13] are included in Table 14 and Fig. 18a, which can also be described adequately with Eq. (26) and $\delta = 4.132 \times 10^{-6}$ cm.

Subsequently, the second hypothesis is considered. From the paste lines it is assumed that if $V_w = V_p \beta_p$, the voids will be completely filled with water, in other words:

$$\phi_p^d = \frac{V_w}{V_w + V_p} = \frac{\beta_p}{\beta_p + 1} \tag{27}$$

In Table 14, this computed void fraction is included. In Table 14 also the ratio of this void content and the void content in loose state is included. This loosely packed void fraction, $\phi_p^1$, of the powders are computed with Eq. (2) and using the powder properties listed in Table 1. For all the powders, it seems that there is constant ratio between both void contents, hence:

$$\phi_p^d = 0.77 \phi_p^1 \tag{28}$$

Apparently, the voids to be filled with water (following from Eq. (27), i.e. from the paste line) are less than present in the same powder when it loosely piled, but there is a constant ratio between them. Upon mixing of the powder with water some compaction will take place, this is the reason this void fraction is assigned with the superscript "d" in Eqs. (27) and (28). It seems that this mixing with water results in a void reduction of about for all powders 23%. Upon vibrating the aggregates, in Section 2 the reduction in void fraction was practically the same. Accordingly, in Fig. 18b the loosely piled void fraction and the compacted void fraction of the three sands and of the gravel, and of the 50% mixes of the three sands and the gravel, taken from Fig. 3, are set out. Furthermore, for the three powders, the void fraction from the loosely piled powder (Table 14) and the void fraction obtained with the paste lines (Eq. (27)) are also included in this figure. Eq. (28), included in this figure as well, matches all values with a good accuracy. Besides these irregularly shaped powders and aggregates, Eq. (28) seems to approach the ratio for spheres as well. For random close packing of uniform spheres, $\phi_p^d = 0.36$ prevails [34,35], whereas for random loose packing of spheres in the limit of zero gravity, $\phi_p^1 = 0.45$ prevails [36].

Now, from the present analysis, one can assess $\beta_p$ as follows:

$$\beta_p = \frac{\phi_p^d}{1 - \phi_p^d} = \frac{\rho_p - \rho_p^d}{\rho_p^d} = \frac{0.77\phi_p^d}{1 - 0.77\phi_p^d} = \frac{0.77\left(\rho_p - \rho_p^1\right)}{\rho_p^1 + 0.23\rho_p} \tag{29}$$

Table 13
Regression results of height capillary rise

| Specimen | Intersection $y$-axis ($H_0$) [mm] | Sorption index (SI) [mm/h$^{0.5}$] | $R^2$ |
|---|---|---|---|
| Mix A, cube 1 | 20.57 | 1.63 | 0.977 |
| Mix A, cube 2 | 21.99 | 1.03 | 0.951 |
| Mix B, cube 1 | 20.69 | 1.54 | 0.988 |
| Mix B, cube 2 | 22.07 | 2.11 | 0.994 |
| Mix C, cube 1 | 20.43 | 1.82 | 0.962 |
| Mix C, cube 2 | 20.39 | 1.89 | 0.985 |

Table 14
Analysis of powders and paste lines (* taken from Domone and Wen [13])

| Material | $S_p$ [cm$^2$/cm$^3$] | $\phi_p^l$ | $\alpha_p$ | $\delta$ [cm] | $\beta_p$ | $\phi_p^d$ | $\phi_p^d/\phi_p^l$ |
|---|---|---|---|---|---|---|---|
| CEM III/B 42.5 N LH/HS | 13,865 | 0.63 | 0.062 | $4.46\times10^{-6}$ | 0.97 | 0.49 | 0.78 |
| Fly ash | 8775 | 0.56 | 0.039 | $4.48\times10^{-6}$ | 0.78 | 0.44 | 0.79 |
| Limestone powder | 12,604 | 0.60 | 0.045 | $3.57\times10^{-6}$ | 0.82 | 0.45 | 0.75 |
| Portland cement* | 11,844 | – | 0.061 | $5.15\times10^{-6}$ | 1.08 | 0.52 | – |
| GGBS* | 12,180 | – | 0.046 | $3.77\times10^{-6}$ | 1.10 | 0.52 | – |

see Eq. (2). Eqs. (26) and (29) enable the computation of $\alpha_p$ and $\beta_p$ for a given powder using its Blaine surface, the particle density and the loosely piled density (or, instead of the latter, the density in compacted state). Domone and Wen [13] demonstrated that these parameters, in turn, are directly related to yield stress and plastic viscosity of the paste.

Note that $\alpha_p$ and $\beta_p$ are the parameters in the *volume* paste line (Eq. (25)). The Chinese Method makes use of

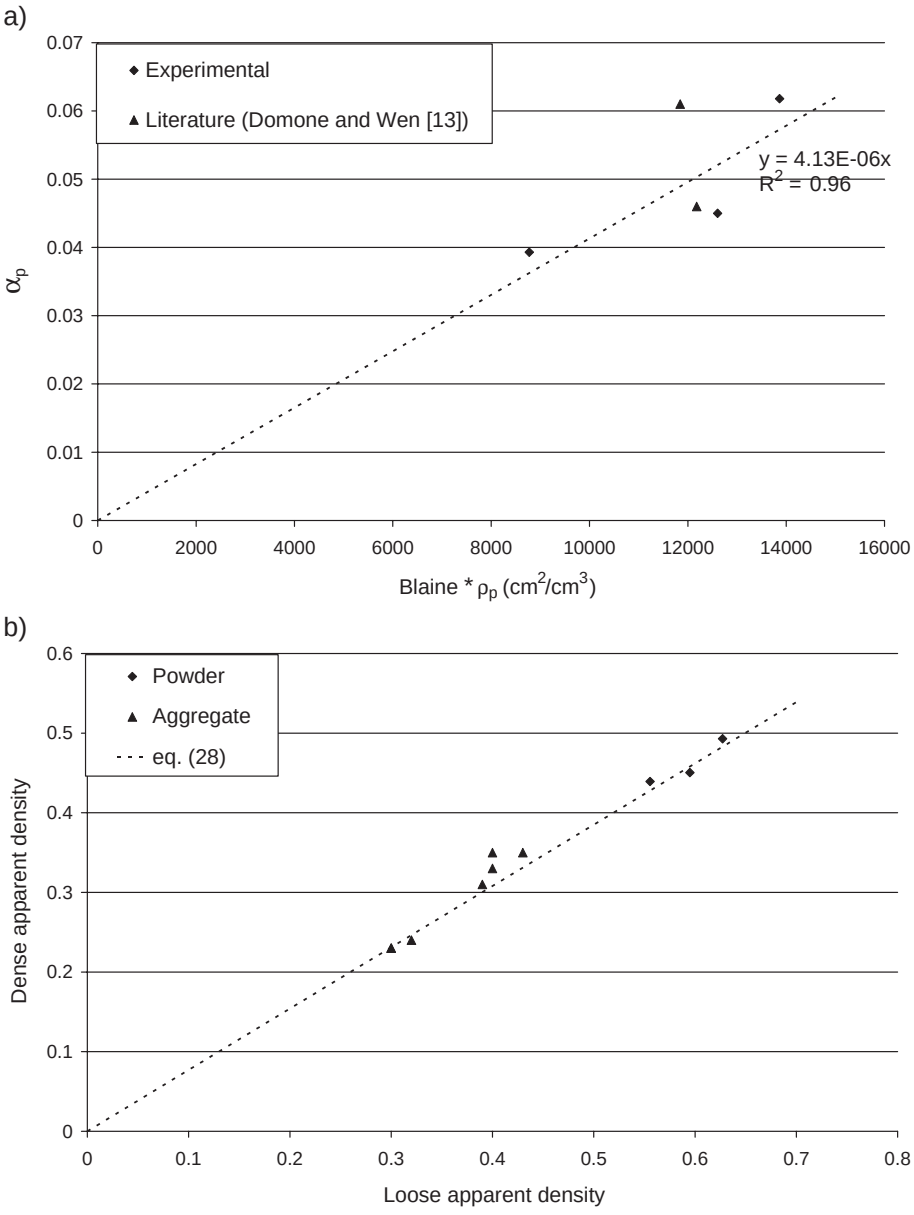


Fig. 18. a) Relation between deformation coefficient from the paste lines and the specific surface of the powder per unit of volume. Data is taken from Table 14. b) Relation between water retention capacity of three powders (from paste lines, Fig. 6 and Table 14) and the void fraction of the loosely piled powders. From the four aggregates the loosely state and compacted state void fractions are also included, as well as of the 50% mixes of the three sands with the gravel (based on data from Fig. 3).

Eqs. (6), (10), (11) and (12), which contain the parameters of the *mass* paste lines. They are related by:

$$a_p = \frac{\rho_w \alpha_p}{\rho_p};\ b_p = \frac{\rho_w \beta_p}{\rho_p} \tag{30}$$

Here, basic relations have been derived for powder–water mixes tested with the Haegermann cone. It is expected that similar basic relations could be derived for concrete mixes and Abrams cone that relate the parameters of slump lines at one hand, with the specific surface area per volume of solid constituents in the mix and their loosely/packed densities at the other hand.

## 9. Conclusions

The Japanese Method makes use of the packed densities of gravel and sand individually, in the Chinese Method the packing of these aggregates is considered integrally. In this study the packing of all solids in the mix (gravel, sand, filler and cement) is considered, which was actually recommended already by Fuller and Thompson ([15], pp. 242–244). Ideally, the grading curve of all solids should follow the modified Andreasen and Andersen curve. Indeed, it followed that the aggregates used by Su et al. [6] and Su and Miao [7] followed this curve (Eq. (13), $q=0.30$). Furthermore, combining the solids, the quantity of paste (water, cement and filler) should be reduced as much as possible. In this paper, it is analysed which combinations of three sands, gravel, SP and slag blended cement result in the lowest powder (cement, limestone powder) content.

Based on these considerations, three mixes have been composed and tested (Table 5) that obey $q=0.25$ as much as possible. Another objective was to meet these theoretical requirements while using the most economical ingredients. This has resulted in three mixes with a low content of powder, ±480 kg/m$^3$ of concrete. The fresh concrete has been evaluated with the Slump-flow, V-funnel and J-ring tests, and its air content has been measured. All mixes meet the criteria set by these tests, whereby the use of superplasticizer could be limited to 1% of the powder content, and the use of a viscosity modifying agent can be avoided.

Up to an age of 28 days, the cured concrete has been tested physically (density, water absorption, etc.) and mechanically (compressive and splitting tensile strengths). The compressive strength tests reveal that the three mixes result in concretes that can be classified as C35/45. The objective of composing medium strength concrete is therefore achieved. It also follows that for the slag cement used (CEM III/B 42.5 N LH/HS), the compressive strength/cement content ratio ($x$) amounts to 0.15 N/mm$^2$ per kg cement/m$^3$ concrete. This measure for the cement efficiency lies within the same range as the values reported by Su et al. [6] and Su and Miao [7]: 0.11–0.14 N/mm$^2$ per kg cement/m$^3$ concrete for Type I Portland Cement. The tensile strength, obtained with the splitting test, appears to be higher than "normal concrete" of comparable compressive strength.

The hardened concrete mixes are also tested on their durability, using both the water intrusion and capillary suction test. Both tests yield that all three mixes can be classified as impermeable and durable. So, using the packing theory of Andreasen and Andersen [9], and its modifications by Funk and Dinger [10] and Elkem [11], cheap SCC mixes can be composed that meet the standards and requirements in fresh and hardened states. Furthermore, a carboxylic polymer type superplasticizer is employed as sole admixture; an auxiliary viscosity enhancing admixture is not needed to obtain the required properties.

Finally, the paste lines are examined and general relations derived. For future application of other powders these relations permit an assessment of the parameters $a_p$ and $b_p$ of the powder (Eqs. (26), (29) and (30)), which in turn can be used to compose the SCC mix (Eqs. (6), (10), (11) and (12)), without the need of cumbersome flow spread tests of the paste. It furthermore follows that the void fraction of both aggregates and powders used are reduced by about 23% upon compaction. This similarity in compaction behaviour could be attributed to the similar (S-) shape PSD of all materials used (Fig. 2).

## List of Symbols

*Roman*

| | |
|---|---|
| $a_p$ | deformation coefficient |
| $b_p$ | retained water ratio |
| $B$ | blocking step [m] |
| $c$ | mass of cement [g] |
| CV | coefficient of variation |
| $d$ | slump [m] |
| dm | dry matter |
| $D$ | particle size [m] |
| $D_{min}$ | minimum particle size [m] |
| $D_{max}$ | maximum particle size [m] |
| $e$ | eccentricity ratio |
| $f_c$ | compressive strength [N/mm$^2$] |
| $f'_{ck}$ | characteristic compressive strength [N/mm$^2$] |
| $f_t$ | tensile strength [N/mm$^2$] |
| $F$ | force [N] |
| $h$ | mix height [m] |
| $H$ | height capillary rise [m] |
| $H_0$ | height capillary rise at $T=0$ [m] |
| $M$ | mass [kg] |
| $m$ | number of specimen |
| $n$ | mass of SP per mass of powder (cement plus filler) |
| $P$ | cumulative finer fraction |
| PF | packing factor |
| $q$ | parameter in (modified) Andreasen and Andersen model |

| | |
|---|---|
| PSD | particle size distribution |
| RH | relative humidity |
| $s$ | standard deviation |
| $S$ | specific surface area per unit of volume [$cm^2/cm^3$] |
| SI | sorption index [$mm/h^{0.5}$] |
| SP | superplasticizer |
| $T$ | time [s] |
| $T_5$ | V-funnel flow out after 5 min [s] |
| $T_{50}$ | time at which the concrete reaches the 50 cm circle [s] |
| $T_s$ | stability time (Eq. (15)) [s] |
| $V$ | volume [$m^3$] |
| $x$ | compressive strength per kg cement/$m^3$ concrete [$Nm^3/kgmm^2$] |
| $z$ | the side of a cube [m] |

*Greek*

| | |
|---|---|
| $\alpha_p$ | deformation coefficient |
| $\beta_p$ | retained water ratio |
| $\beta$ | parameter (Eq. (17)) |
| $\delta$ | parameter [cm] |
| $\varphi$ | void fraction |
| $\rho$ | density [$g/cm^3$] |
| $\Gamma$ | relative slump |

*Subscript*

| | |
|---|---|
| a | aggregate |
| air | air |
| c | cement |
| cube | cube |
| f | filler (fly ash, stone powder) |
| m | mortar |
| p | powder (cement, filler) |
| tot | total |
| w | water |

*Superscript*

| | |
|---|---|
| air | in air |
| d | densely packed |
| water | underwater |
| l | loosely packed |
| SCC | Self-Compacting Concrete |
| - | mean |

## Acknowledgements

The authors would like to express their gratitude to Mrs. Ir. W.J. Bouwmeester-Van den Bos, Ing. H. ter Welle, Mr. B. Bos and Mr. B. Piscaer for their advice. They furthermore would like to thank their colleagues Ing. G.H. Snellink and Mr. H.M. Menkehorst for the laboratory support. The authors furthermore wish to thank the following institutions for their financial support of the Cement-Concrete-Immobilisates Research: Cornelis Lely Foundation, Delta Marine Consultants, Betoncentrale Twenthe, Rokramix, Dutch Ministry of Infrastructure, Senter Novem Soil, Jaartsveld Groen en Milieu.

## References

[1] H. Okamura, Self-compacting High-Performance Concrete, Concrete International 19 (7) (1997) 50–54.
[2] H. Okamura, M. Ouchi, Self-Compacting Concrete—development, present, and future, RILEM, Proc. 1st International RILEM Symposium on Self-Compacting Concrete, 1999, pp. 3–14.
[3] H. Ter Welle, Betoncentrale Twenthe, Hengelo, The Netherlands, Personal communications (2003).
[4] B. Bos, BAS, Venray, The Netherlands, Personal communications (2003).
[5] F.M.L. Ernst, Onderzoek zelfverdichtend beton. MSc Thesis TUE/CCO/00-09, Eindhoven University of Technology, Faculteit Bouwkunde, Capaciteitsgroep Constructief Ontwerpen, Eindhoven, The Netherlands, 2000 (in Dutch).
[6] N. Su, K.C. Hsu, H.W. Chai, A simple mix design method for Self-Compacting Concrete, Cement and Concrete Research 31 (2001) 1799–1807.
[7] N. Su, B. Miao, A new method for mix design of medium strength concrete with low cement content, Cement & Concrete Composites 25 (2003) 215–222.
[8] A.M. Neville, Properties of Concrete, 4th ed., Prentice Hall/Pearson, Harlow, 2000.
[9] A.H.M. Andreasen, J. Andersen, Ueber die Beziehung zwischen Kornabstufung und Zwischenraum in Produkten aus losen Körnern (mit einigen Experimenten), Kolloid-Zeitschrift 50 (1930) 217–228 (in German).
[10] J.E. Funk, D.R. Dinger, Predictive Process Control of Crowded Particulate Suspension, Applied to Ceramic Manufacturing, Kluwer Academic Press, 1994.
[11] Elkem Materials, User Documentation Language Independent Size Distribution Analyser (L.I.S.A), http://www.refractories.elkem.com (2003).
[12] H.J. Radix, Chinese mengselontwerpmethode voor Zelfverdichtend Beton; Onderzoek naar goedkope ZVB mengsels met normale druksterkte, op basis van een nieuwe ontwerpmethode en de toepassing van fijn zand. MSc thesis, University of Twente, Faculty of Engineering Technology, The Netherlands, 2004 (in Dutch).
[13] P. Domone, C.H. Wen, Testing of binders for High Performance Concrete, Cement and Concrete Research 27 (1997) 1141–1147.
[14] Dutch Normalization-Institute, NEN 5950:1995 Voorschriften Beton Technologie. Eisen, vervaardiging en keuring, Nederlands Normalisatie Instituut, Delft, The Netherlands, 1995, (in Dutch).
[15] W.B. Fuller, S.E. Thompson, The laws of proportioning concrete, Transactions of the American Society of Civil Engineers 33 (1907) 222–298.
[16] A.M. Gaudin, An investigation of crushing phenomena, Petroleum Development and Technology 73 (1926) 253–316.
[17] BFBN, Cursushandboek Zelfverdichtend Beton, Bond van Fabrikanten van Betonproducten in Nederland (BFBN), Woerden, The Netherlands, 2001, (in Dutch).
[18] EFNARC, Specification and Guidelines for Self-Compacting Concrete. EFNARC (European Federation of Producers and Applicators of Specialist Products for Structures), 2002 (February). http://www.efnarc.org/pdf/SandGforSCC.PDF.
[19] S.F.A. Ankoné, Zelfverdichtend Beton. Training Period Report, University of Twente, Faculty of Engineering Technology, The Netherlands, 2000, (in Dutch).
[20] J.C. Walraven, K. Takada, G.I. Pelova, Zelfverdichtend beton, hoe maak je dat?, Cement (The Netherlands) 3 (1999) 68–72 (in Dutch).

[21] CUR, CUR-Aanbeveling 93, Zelfverdichtend Beton, Stichting CUR, Gouda, The Netherlands, 2002, (in Dutch).
[22] BMC, Aanvulling BRL 1801, Aanvulling op de Nationale Beoordelingsrichtlijn Betonmortel (BRL 1801), Hoogvloeibare, verdichtingsarme en zelfverdichtende betonmortel. Certificatie Instelling Stichting BMC, Gouda, The Netherlands, 2002. http://www.bmc-cert.nl/nederlands/brl/1801_aanvulling_zvb.pdf (in Dutch).
[23] H.W. Reinhardt, DAfStb guideline on self compacting concrete, BFT (Beton+Fertigteil–Technik) 67 (12) (2001) 54–62.
[24] S. Hanehara, K. Yamada, Interaction between cement and chemical admixture from the point of cement hydration, adsorption behaviour of admixture, and paste rheology, Cement and Concrete Research 29 (1999) 1159–1165.
[25] Dutch Normalization-Institute, NEN5962:1999 Beton en mortel—Bepaling van het luchtgehalte van beton- en mortelspecie met niet-poreus toeslagmateriaal (drukmethode), Nederlands Normalisatie-Instituut, Delft, The Netherlands, 1999, (in Dutch).
[26] H.J.H. Brouwers, On the particle size distribution and void fraction of polydisperse random packings, CE&M Research Report, University of Twente, Enschede, The Netherlands (in press).
[27] Dutch Normalization-Institute, NEN5967:1988 Beton—Bepaling van de volumieke massa, Nederlands Normalisatie-Instituut, Delft, The Netherlands, 1988, (in Dutch).
[28] Dutch Normalization-Institute, NEN5968:1988 Beton en mortel—Bepaling van de druksterkte van proefstukken, Nederlands Normalisatie-Instituut, Delft, The Netherlands, 1988, (in Dutch).
[29] Dutch Normalization-Institute, NEN5969:1988 Beton en mortel—Bepaling van de splijttreksterkte van proefstukken, Nederlands Normalisatie-Instituut, Delft, The Netherlands, 1988, (in Dutch).
[30] Dutch Normalization-Institute, NEN6722:1989 Voorschriften Beton Uitvoering, Nederlands Normalisatie-Instituut, Delft, The Netherlands, 1989, (in Dutch).
[31] Dutch Normalization-Institute, NEN-EN12390-8:2000 Beproeven van verhard beton—Deel 8: Indringingsdiepte van water onder druk, Nederlands Normalisatie-Instituut, Delft, The Netherlands, 2000, (in Dutch).
[32] K. Audenaert, V. Boel, G. de Schutter, Water permeability of self compacting concrete, Proc. 11th ICCC (3), 2003, pp. 1574–1583.
[33] W. Zhu, P.J.M. Bartos, Permeation properties of Self-Compacting Concrete, Cement and Concrete Research 33 (2003) 921–926.
[34] G.D. Scott, Packing of equal spheres, Nature 188 (1960) 908–909.
[35] G.D. Scott, D.M. Kilgour, The density of random close packing of spheres, Brit. J. Appl. Phys. (J. Phys. D), vol. 2, 1969, pp. 863–866.
[36] G.Y. Onoda, E.G. Liniger, Random loose packings of uniform spheres and the dilatancy onset, Physical Review Letters 64 (1990) 2727–2730.

Available online at www.sciencedirect.com
ScienceDirect
Cement and Concrete Research 37 (2007) 1376
Cement and Concrete Research

Erratum

# Erratum to "Self-Compacting Concrete: Theoretical and experimental study" [Cement and Concrete Research 35(11) (2005) 2116–2136]

H.J.H. Brouwers *, H.J. Radix

*Department of Civil Engineering, Faculty of Engineering Technology, University of Twente, P.O. Box 217, 7500 AE Enschede, The Netherlands*

Received 21 May 2007; accepted 22 May 2007

In Cement and Concrete Research 35, 2116–2136 (2005), Self-compacting concrete: theoretical and experimental study, by H.J.H. Brouwers and H.J. Radix, Eqs. (10) and (29) should be replaced by

$$V_f = \frac{\phi^{SCC} \cdot m^3 - V_{air} - V_c\left(1 + \left(a_c \Gamma_p + b_c\right)\frac{\rho_c}{\rho_w} + dm_{SP} \cdot n \cdot \frac{\rho_c}{\rho_{SP}}\right)}{1 + \left(a_f \Gamma_P + b_f\right)\frac{\rho_f}{\rho_w} + dm_{SP} \cdot n \cdot \frac{\rho_f}{\rho_{SP}}}, \tag{10}$$

and

$$\beta_p = \frac{\varphi_p^d}{1 - \varphi_p^d} = \frac{0.77 \cdot \varphi_p^l}{1 - 0.77 \cdot \varphi_p^l} = \frac{0.77 \cdot \left(\rho_p - \rho_p^l\right)}{0.77 \cdot \rho_p^l + 0.23 \cdot \rho_p}, \tag{29}$$

respectively. The typological errors have no further impact on the content of the paper.

In Section 8, all appearing $\phi$ should be replaced by $\varphi$. In the captions of Figs. 11 and 12, "mass" should be replaced by "volume".

## Acknowledgement

The authors wish to thank Mr. L. Kraft from Norut Teknologi AS, Narvik, Norway for retrieving the errors.

DOI of original article: 10.1016/j.cemconres.2005.06.002.
* Corresponding author.
*E-mail address:* h.j.h.brouwers@utwente.nl (H.J.H. Brouwers).

0008-8846/$ - see front matter 
doi:10.1016/j.cemconres.2007.05.004